UC Irvine
UC Irvine Previously Published Works

Title

Reconfigurations within resonating communities of brain regions following TMS reveal different scales of processing.

Permalink

https://escholarship.org/uc/item/0f83b94x

Journal

Network Neuroscience, 4(3)

Authors

Garcia, Javier
Ashourvan, Arian
Thurman, Steven
et al.

Publication Date

2020

DOI

10.1162/netn_a_00139

Copyright Information

This work is made available under the terms of a Creative Commons Attribution License, available at https://creativecommons.org/licenses/by/4.0/

Peer reviewed

eScholarship.org Powered by the California Digital Library
University of California

NETWORK NEUROSCIENCE

an open access journal

Check for updates

Citation: Garcia, J. O., Ashourvan, A., Thurman, S. M., Srinivasan, R., Bassett, D. S., & Vettel, J. M. (2020). Reconfigurations within resonating communities of brain regions following TMS reveal different scales of processing. *Network Neuroscience*, *4*(3), 611–636. https://doi.org/10.1162/netn_a_00139

DOI:
https://doi.org/10.1162/netn_a_00139

Supporting Information:
https://doi.org/10.1162/netn_a_00139

Received: 10 September 2019
Accepted: 23 March 2020

Competing Interests: The authors have declared that no competing interests exist.

Corresponding Author:
Javier Omar Garcia
javier.o.garcia.civ@mail.mil

Handling Editor:
Martijn van den Heuvel

Copyright: No rights reserved. This work was authored as part of the Contributors official duties as an Employee of the United States Government and is therefore the work of the United States Government. In accordance with 17 U.S.C. 105, no copyright protection is available for such works under U.S. law.

The MIT Press

RESEARCH

Reconfigurations within resonating communities of brain regions following TMS reveal different scales of processing

Javier O. Garcia[1,2], **Arian Ashourvan**[1,2], **Steven M. Thurman**[1], **Ramesh Srinivasan**[3,4], **Danielle S. Bassett**[2,5], **and Jean M. Vettel**[1,2,6]

[1]U.S. Army CCDC Army Research Laboratory, Aberdeen Proving Ground, MD, USA

[2]Department of Bioengineering, University of Pennsylvania, Philadelphia, PA, USA

[3]Department of Cognitive Sciences, University of California, Irvine, Irvine, CA, USA

[4]Department of Biomedical Engineering, University of California, Irvine, Irvine, CA, USA

[5]Department of Electrical and Systems Engineering, University of Pennsylvania, Philadelphia, PA, USA

[6]Psychological and Brain Sciences, University of California, Santa Barbara, Santa Barbara, CA, USA

Keywords: Neuroimaging, Network flexibility, Network allegiance, Local-global processing, TMS, EEG

ABSTRACT

An overarching goal of neuroscience research is to understand how heterogeneous neuronal ensembles cohere into networks of coordinated activity to support cognition. To investigate how local activity harmonizes with global signals, we measured electroencephalography (EEG) while single pulses of transcranial magnetic stimulation (TMS) perturbed occipital and parietal cortices. We estimate the rapid network reconfigurations in dynamic network communities within specific frequency bands of the EEG, and characterize two distinct features of network reconfiguration, flexibility and allegiance, among spatially distributed neural sources following TMS. Using distance from the stimulation site to infer local and global effects, we find that alpha activity (8–12 Hz) reflects concurrent local and global effects on network dynamics. Pairwise allegiance of brain regions to communities on average increased near the stimulation site, whereas TMS-induced changes to flexibility were generally invariant to distance and stimulation site. In contrast, communities within the beta (13–20 Hz) band demonstrated a high level of spatial specificity, particularly within a cluster comprising paracentral areas. Together, these results suggest that focal magnetic neurostimulation to distinct cortical sites can help identify both local and global effects on brain network dynamics, and highlight fundamental differences in the manifestation of network reconfigurations within alpha and beta frequency bands.

AUTHOR SUMMARY

TMS may be used to probe the causal link between local regional activity and global brain dynamics. Using simultaneous TMS-EEG and dynamic community detection, we introduce what we call "resonating communities" or frequency band-specific clusters in the brain, as a way to index local and global processing. These resonating communities within the alpha and beta bands display both global (or integrating) behavior and local specificity, highlighting fundamental differences in the manifestation of network reconfigurations.

INTRODUCTION

The brain is an intricate collection of heterogeneous areas (Alivisatos et al., 2012), and a central goal of neuroscientific research is to understand how the coordination of these different regions supports cognition (Azevedo et al., 2009; Bressler & Menon, 2010; Gollo, Roberts, & Cocchi, 2017). One theoretical approach encapsulates the coordinated activity into a framework of scales, and research has examined how local regional activity harmonizes with global signals (Bressler & Kelso, 2001). Local activity refers to cortical or thalamocortical interactions that reflect the transient coordination of inhibitory and excitatory neighboring neurons, constrained by basic neurophysiological factors such as refractory limitations and synaptic rising (Fries, Nikolić, & Singer, 2007). However, research has shown that this local neural activity can also be modulated by global activity in the brain (for review, see Buzsáki & Draguhn, 2004; Buzsáki & Wang, 2012). Global activity arises from propagation delays in cortico-cortical fibers and reflects the dynamic interactions and synchronization among distal networks. This conceptual framework of local and global networks interacting in cognitive processes is critical to the interpretation of neurophysiological signals. Yet, how this activity coheres to manifest cognition is still an active area of study (Bressler & Kelso, 2001; Cocchi, Gollo, Zalesky, & Breakspear, 2017).

Electroencephalography (EEG): A method to monitor electrical activity emanating from the brain but recorded from the scalp.

EEG affords a natural way to study the scales of processing by examining oscillatory dynamics in different frequency bands (Buzsáki & Draguhn, 2004; Canolty & Knight, 2010). Changes in power in high frequencies, such as beta and gamma, have been used to infer local dynamics arising from the synchronization of populations of neurons (Brunel & Wang, 2003; Geisler, Brunel, & Wang, 2005). Similarly, the emergent activity in slower EEG frequencies, ranging across delta, theta, and alpha, has been interpreted as global activity arising from long-distance coordination of synchronized neural firing in disparate brain regions (Brunel & Wang, 2003; Geisler et al., 2005); however, there are known examples of cross-frequency interactions that challenge a strict local/global interpretation on frequency dynamics (Canolty & Knight, 2010). Together, results from EEG studies have indicated the importance of both local and global activity, indexed by high- and low-frequency oscillations, for understanding variability in human behavior (Buzsáki, 2006; Nunez & Srinivasan, 2006; Nunez, Wingeier, & Silberstein, 2001; Volberg, Kliegl, Hanslmayr, & Greenlee, 2009). However, EEG provides only an inferential framework to study interactions across scales of neural activity. Advancements in neurostimulation paradigms may provide an avenue to directly study the causal role of local changes in oscillatory dynamics on global dynamics (Bergmann, Karabanov, Hartwigsen, Thielscher, & Siebner, 2016; Pascual-Leone, Walsh, & Rothwell, 2000), a long-known property of neurostimulation (Ilmoniemi et al., 1997).

Transcranial magnetic stimulation (TMS): A type of brain stimulation that noninvasively introduces electrical current into the brain to perturb neural activity.

Transcranial magnetic stimulation (TMS) has been proposed as a method to actively probe the dynamic interplay between local processing and consequent global interactions with more distal regions of the brain (Massimini, Tononi, & Huber, 2009; Romei, Thut, Mok, Schyns, & Driver, 2012). Traditionally, single-pulse TMS is a technique used to induce a short, controlled burst of activity in a predetermined local brain region, directly causing a change in the local dynamics (Pascual-Leone et al., 2000). Research has identified behavioral outcomes resulting from local stimulation for patients in clinical settings and healthy individuals in experimental tasks. For example, local stimulation in patients can successfully determine stroke recovery (for review, see Auriat, Neva, Peters, Ferris, & Boyd, 2015), mitigate severe affective disorders (e.g., Berman et al., 2000), and preserve motor and language functions in presurgical mapping (Eldaief, Press, & Pascual-Leone, 2013). TMS has also been successfully employed to confirm the role of an individual brain region on task performance, ranging from sensory attention (Herring, Thut, Jensen, & Bergmann, 2015; Romei, Murray, Cappe, & Thut, 2013; Taylor & Thut, 2012) to working memory performance (Brunoni & Vanderhasselt, 2014;

Rose et al., 2016). Yet, extant experimental research has also demonstrated that the brain alterations caused by TMS are not limited to local perturbations (Ilmoniemi et al., 1997; Sale, Mattingley, Zalesky, & Cocchi, 2015). By pairing TMS with other concurrent imaging modalities like EEG, it provides an innovative approach to study connectivity relationships among disparate brain regions (Cocchi et al., 2015; Mancini et al., 2017; Siebner et al., 2009).

Multimodal studies have paired TMS with functional neuroimaging, such as fMRI (e.g., Bestmann et al., 2008; Bohning et al., 1999), EEG (e.g., Bortoletto, Veniero, Thut, & Miniussi, 2015; Garcia, Grossman, & Srinivasan, 2011), and PET (e.g., Paus, 1998), and measured stimulation-induced responses in brain areas that are distal to the stimulation site, indicating that stimulation can induce transient coordination between local and global activity (Bestmann et al., 2008; Driver, Blankenburg, Bestmann, Vanduffel, & Ruff, 2009; Paus, 1998). Complementing these findings, computational models of neurodynamics have demonstrated that regional differences in structural connectivity may provide a mechanistic account for how local network activity that is induced from a focal TMS pulse can propagate along cortico-cortical fibers to influence global network synchronization (Gollo et al., 2017; Muldoon et al., 2016). This idea is supported by neurostimulation research that shows a structure-function constraint to the local stimulation and subsequent global (de)synchronization (Amico et al., 2017). While both experimental and modeling work have suggested the importance of interacting networks, few studies have employed the rich set of tools of network science to understand the propagation of TMS stimulation throughout the brain (Bortoletto et al., 2015). Network science not only provides a mathematical language to describe complex connectivity patterns resulting from stimulation; previous research has also proposed a variety of summary metrics in which to characterize local and global connectivity in the brain (for review, see Garcia, Ashourvan, Muldoon, Vettel, & Bassett, 2018). In this study, we address this existing gap in the literature and employ a method recently developed in network science to study the interactions of local connectivity and global network dynamics following TMS stimulation.

We investigated network reconfigurations from resting-state EEG following single pulses of transcranial magnetic stimulation using a method from network science that reveals modular architecture in the brain (Bassett & Bullmore, 2006; Bullmore & Sporns, 2012; Ercsey-Ravasz et al., 2013). Participants received single pulses of TMS to occipital or parietal cortex, and we computed functional connectivity using EEG data for a 2-s epoch surrounding stimulation (−1 to 1). Our theoretical question focused on the comparison of stimulations to spatially disparate, large lobes of the brain, investigating how stimulation influenced network dynamics following stimulation as indexed by the modular architecture of the functional connectivity patterns. Each module is composed of regions with synchronized activity that are thought to be dynamically linked for the purpose of cohesive processing (Achard, Salvador, Whitcher, Suckling, & Bullmore, 2006; Bassett & Bullmore, 2006; Sporns, Chialvo, Kaiser, & Hilgetag, 2004). To index local and global activity, we investigate two frequency bands that probe brain dynamics across these scales. We separately characterize the modular architecture of resting-state EEG within the alpha band and within the beta band, from which we define *resonating communities*, or communities of brain regions restricted to each frequency band. This delineation was inspired, in part, by the theoretical proposal by Rosanova et al. (2009) that posits that brain regions have a primary natural frequency: Resting-state activity is dominated by alpha in the occipital cortex, whereas parietal activity is dominated by beta activity. Consequently, we hypothesized that network changes in these frequency bands would both differentiate the location of the stimulation site (occipital vs. parietal), and reveal the spatial scale (local vs. global) of the propagation of network perturbations arising from TMS.

Resonating communities (or clusters): Cluster of brain nodes representing a network defined by band-specific oscillatory activity (e.g., alpha activity).

Module allegiance:
A metric derived from a series of node labels (i.e., network affiliation) that indicates how often nodes are within the same network of other nodes.

Network flexibility:
A metric derived from a series of labels that reveals how often a node changes its network affiliation across time.

To characterize changes in functional network organization before and after stimulation, we used two well-established metrics from network science: *module allegiance* and *network flexibility*. Allegiance estimates how often regions are functionally connected with other regions, capturing stable subnetworks in the community structure across time points. Flexibility, in contrast, reveals the extent to which a region frequently (and flexibly) changes its assignment across communities between time points. Thus, allegiance is a construct that can capture coordinated activity of each node with every other node in the brain, thereby increasing the resolution of community assignments, whereas flexibility reveals the propensity of brain regions to change affiliations overall. We argue that these complementary metrics are uniquely suited to investigate the scale of processing effects of stimulation since allegiance captures the unique shifts between each *pair* of regions and flexibility identifies whether a node tends to shift its community affiliation over time. Our analyses extend previous research that has found that network flexibility successfully characterizes *large-scale functional differences* (e.g., Telesford et al., 2016), for example in executive function (Braun et al., 2015) and mood (Betzel, Satterthwaite, Gold, & Bassett, 2017). Allegiance, on the other hand, has been used to describe *observed network dynamics on a finer scale*, estimating alignment with a predefined functional architecture (Bassett et al., 2015) as well as identifying transitions among certain network configurations (Ashourvan, Gu, Mattar, Vettel, & Bassett, 2017). Across the set of network science metrics adapted for neuroscience application (for review, see Garcia et al., 2018), allegiance and flexibility are the best suited to identify changes in scales of processing.

Using these measures, we report substantial differences between the alpha and beta band communities. While activity in the alpha network revealed a dynamic interplay of local and global connectivity, as hypothesized, communities within the beta band displayed a spatial specificity across both metrics, suggesting a more *local* connectivity impact of stimulation. Together, these results show how focal TMS to distinct cortical sites can help reveal both local and global effects on dynamic network configurations, and demonstrate fundamental differences in the manifestation of network effects in alpha and beta frequency bands in different areas of the brain.

RESULTS

Here we studied the brain dynamics following single pulses of TMS to occipital and parietal cortex using recently developed approaches from network science. First, TMS was delivered to two separate sites and we focused our analysis on two separate frequency bands. Next, because of the artifact-prone simultaneous technique of TMS-EEG (Rogasch & Fitzgerald, 2013), we took several precautions and used strict criteria to reduce the measured artifact (see the Materials and Methods section). We then reconstructed estimated neural sources on a volumetric brain mesh and then extracted time series for 68 brain regions (Figure 1). Using epochs surrounding the stimulation period, we computed functional connectivity between all region pairs using the debiased weighted phase lag index (dwPLI) that has shown robustness to noise (Vinck, Oostenveld, van Wingerden, Battaglia, & Pennartz, 2011;Vindiola, Vettel, Gordon, Franaszczuk, & McDowell, 2014). Our analysis focused on connectivity in the alpha and beta frequency bands since these bands have been suggested as resonant frequencies within the stimulated regions, alpha in occipital and beta in parietal regions (Laufs et al., 2003; Rosanova et al., 2009). We interpret our results within this context, and while our results converge to a narrative of local/global dynamics across frequency bands, we also must consider potential confound to these techniques (e.g., auditory responses, muscle contractions, and the like; for review, see Rogasch & Fitzgerald, 2013).

Debiased weighted phase lag index (dwPLI):
A specific type of functional connectivity, often used in EEG analysis, that is specifically designed to estimate the nodal interrelationship with little artifact interference.

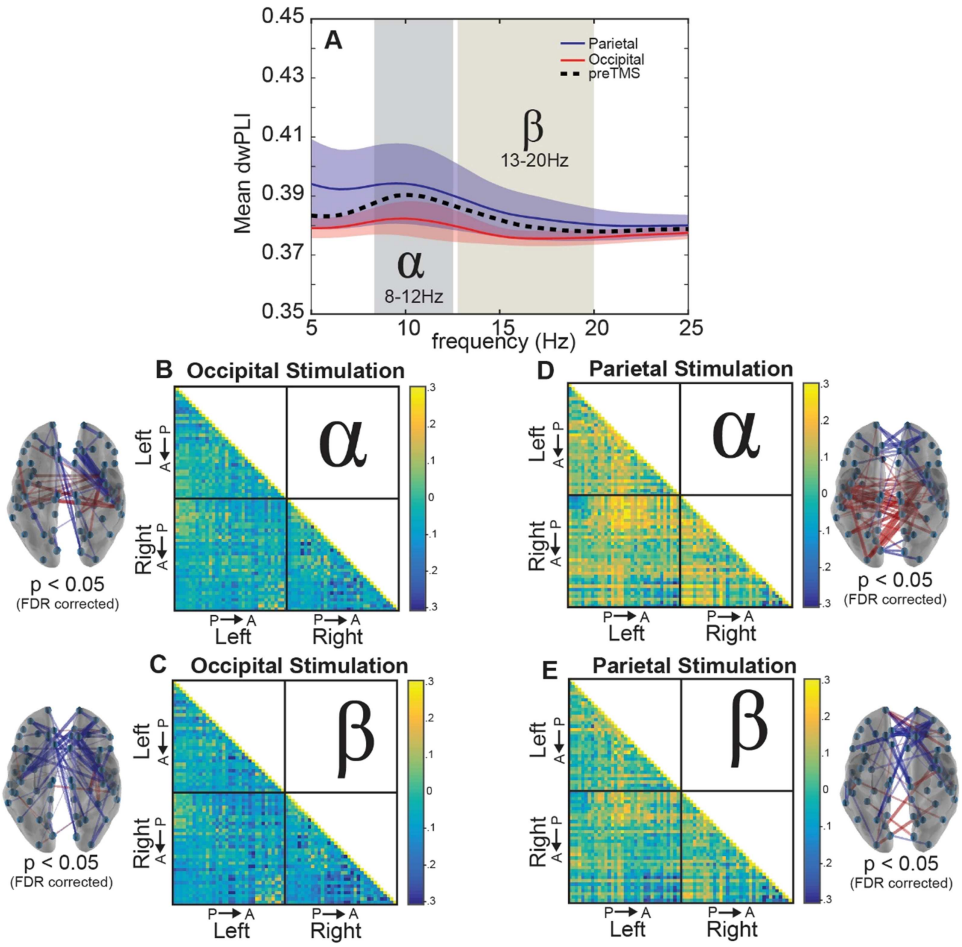

Figure 1. Whole-brain connectivity changes following stimulation. (A) Average dwPLI across the brain between 5 Hz and 25 Hz. (B, C) Debiased weighted phase lag index (dwPLI) differences between the second after TMS (post-TMS) and the second before TMS (pre-TMS) intervals across trials averaged for occipital stimulation within the alpha band (B) and beta band (C). (D, E) Results similar to Panels B and C, but for parietal stimulation. Brain insets display the significant connections ($p < 0.05$, FDR adjusted) across the brain, providing a topographical illustration of the connectivity matrices where red lines indicate increased connectivity following stimulation and blue lines indicate decreased connectivity following stimulation.

Stimulation Effects on Whole-Brain Connectivity

We began by examining patterns of functional connectivity in a whole-brain analysis (see Figure 1). We observed slightly higher connectivity across the brain within the alpha band (8–12 Hz) both before (black dotted line in Figure 1A) and after stimulation to either site in bilateral occipital cortex (red line) or bilateral parietal cortex (blue line) compared with other frequency bands. This dominant response in whole-brain alpha synchrony likely reflects its role as a diffuse, communicative signal with multiple functions (Başar, Başar-Eroğlu, Karakaş, & Schürmann, 1999), serving as a global signal for sensory and information processing.

We next investigated changes in connectivity following stimulation by comparing changes between pre- and post-TMS intervals. As shown in Figure 1A, we observed that the average connectivity between all region pairs did not show much change within the alpha band after

stimulation to either occipital or parietal sites (occipital: $t(9) = -0.95$, $p = 0.36$; parietal: $t(9) = 1.05$, $p = 0.32$, all uncorrected), and this was mirrored in the beta band with minimal connectivity differences for both stimulation locations (occipital: $t(9) = -1.39$, $p = 0.20$; parietal: $t(9) = 0.41$, $p = 0.69$, all uncorrected). However, there was a marked difference between occipital and parietal stimulation sites when examining the directionality and spatial specificity of the change following stimulation (Figure 1B–E). We submitted the difference in the average dwPLI estimate 1 s after the TMS pulse to that before the TMS pulse using a one-sample t test and then adjusted for multiple comparisons via false discovery rate (q; Benjamini & Yekutieli, 2001). By subtracting the post-TMS dwPLI estimate from the pre-TMS baseline, we observed a dispersed global decrease in connectivity for occipital stimulation (Figure 1B–C) for the regional pairs with the largest differences within the alpha and beta bands. Significant connections show some regional specificity, where the beta band shows decreases in connectivity between lateral central locations and medial frontal sites ($q < 0.05$). The alpha band shows a similar connectivity pattern with an additional increase in connectivity between lateral regions toward the center of the brain. In contrast, we observed a marked increase within central and parietal sites as well as a frontal decrease in connectivity for parietal stimulation ($q < 0.05$; Figure 1D–E). The alpha band shows a significant pattern of connectivity increases along in parietal regions ($q < 0.05$), but this pattern is less robust within the beta band. Collectively, these whole-brain connectivity results show some frequency specificity for the stimulation sites, as might be predicted based on theories that suggest that stimulation could be facilitated or decremented by the inherent resonant frequency of the tissue (Rosanova et al., 2009) and a difference between stimulation sites as well. Since these connectivity results show both site and frequency specificity and generality from stimulation, it is possible that a portion of these results (the pattern that is similar across the stimulation sites and oscillations of interest) is driven by confounding variables (for review, see Rogasch & Fitzgerald, 2013), despite the extreme caution taken in artifact reduction (see the Materials and Methods section). Nevertheless, this observation could reflect the global influence of these regions on whole-brain connectivity rather than their targeted effects on subnetworks. Consequently, we next employed recent methods from network science to examine the effect of stimulation at a finer scale than average connectivity across nodes.

Community Organization in Resting Networks

To examine stimulation effects in brain communities, we capitalized on a network science approach that has been used previously to study modularity in brain networks. To estimate dynamic community structure, we optimize a multilayer modularity quality function, Q, using a Louvain-like greedy algorithm (Blondel, Guillaume, Lambiotte, & Lefebvre, 2008; Mucha, Richardson, Macon, Porter, & Onnela, 2010) to assign brain regions to communities, where each layer is a separate time slice. With this optimization, we extract our experimental *communities* by finding an optimal parameter scheme, which is composed of two parameters: (a) a structural resolution γ parameter and (b) a temporal resolution ω parameter. These two parameters determine the scale of the resulting graph, both structurally and temporally. As described in Garcia et al. (2018), there are several heuristics we may use to determine the optimal parameter for our dataset. We chose an unbiased "difference" heuristic because of the unique properties of this stimulation dataset. With this method, we compare the estimated Q from the pre-TMS interval to a Qnull derived from a shuffled null connectivity matrix where we shuffle the pairwise dwPLI values, destroying the correlational structure observed in EEG data for each subject and parameter pairing. Each Q was then subtracted for each parameter pairing, comparing the observed model's Q (from the unperturbed EEG connectivity patterns)

and the null model's Qnull (shuffled connectivity patterns) for each subject; our analysis found a clear peak in the resulting Q matrix, suggesting that the range used was appropriate for this dataset.

This data-driven approach showed more local granularity in the network landscape following stimulation. Importantly, we defined network communities without stimulation during a period of rest. This allowed us to interrogate the dynamics of community reconfigurations following TMS, given a natural baseline, unbiased by the stimulation itself. Importantly, however, we interpret our results both within the confines of this community organization (Figures 3 and 4) and outside of these confines (Figure 5). We defined network communities separately for both the alpha and beta bands, and used the most robust arrangement across the 100 iterations of modularity maximization as the final community structure. The 100 iterations of the pre-TMS interval were remarkably robust and consistent, showing 100% agreement across iterations for the alpha band and 98% agreement across the iterations within the beta band. We also observed noteworthy similarity (approximately 97% spatial similarity) between them except for a small cluster of motor-related brain regions (Figure 2).

In the alpha band (Figure 2, left), five communities are illustrated: a bilateral occipital-parietal network (Occ, blue); a right paracentral community (RPC, pink); a left temporal network (LTem, yellow); a right temporal network (RTem, green); and a bilateral frontal network (Fron, orange). This largest community (Occ) is a large cluster of regions in occipital and parietal cortex, an organization that is perhaps unsurprising, given the commonly observed peak of the alpha rhythm within occipital-parietal regions (Hari & Salmelin, 1997). Interestingly, five similar communities were also found within the beta band (Figure 2, right), and the only observed difference was in the right paracentral community (Desikan-Killiany atlas regions: R precentral, R postcentral). In addition to the two nodes of the pre- and postcentral sulcus in the alpha RPC community, the beta band RPC community also contained regions of the medial paracentral lobule, putative sources of motor-related planning (Desikan-Killiany atlas regions:

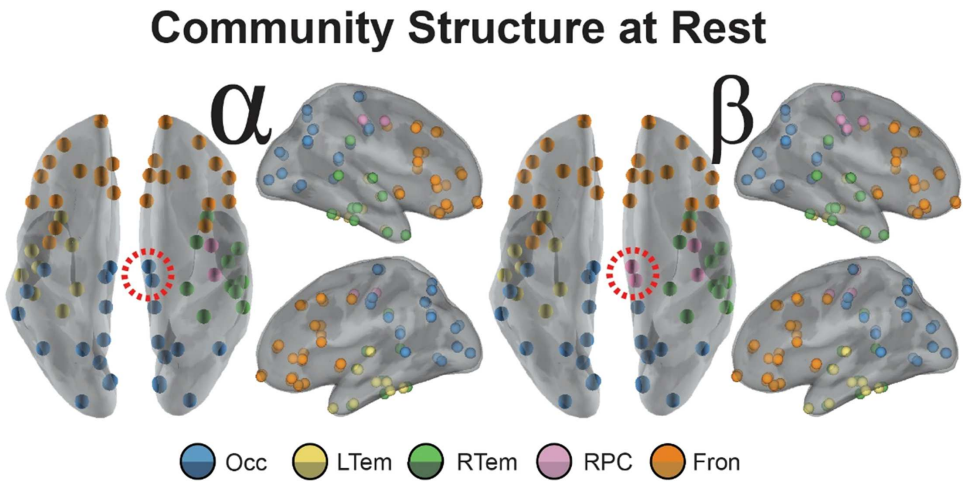

Figure 2. Communities derived from the interregional allegiance matrix in the pre-TMS interval for the alpha and beta bands. Inflated mesh visualizations of brain regions colored by community organization. Orbs are plotted at the centroid of the regions of interest. Community organization was found independently for the alpha band (left) and beta band (right) before stimulation with TMS. Dotted lines surrounding nodes near medial portion of the brains indicate the only two nodes unique to the different frequency bands.

R paracentral, R posterior cingulate). This RPC community in beta nicely aligns with previous literature that implicates the beta band in motor-related activity (**?**), providing support that the detected network communities captured frequency-specific effects.

Community Allegiance Differentiates Beta Band Communities From the Alpha Band

We next sought to characterize how stimulation influenced dynamic network reconfigurations from the natural baseline resting state. We employed a metric of allegiance that captures how often two nodes are present within the same community before and after stimulation. Figure 3 (A, C) shows the average pairwise difference in allegiance before and after stimulation within each of the five communities identified from the pre-TMS resting-state connectivity ($\text{Alleg}_{\text{post}} - \text{Alleg}_{\text{pre}}$). Within the alpha band (top row), we observe some specificity to the stimulation site. In comparing allegiance for each pairing of the communities, allegiance change is highest for the occipital-parietal community (Occ) and lowest for the frontal community (Fron; paired t test, $t(9) = 3.8$, $p = 0.004$, uncorrected), and this was true for each of the

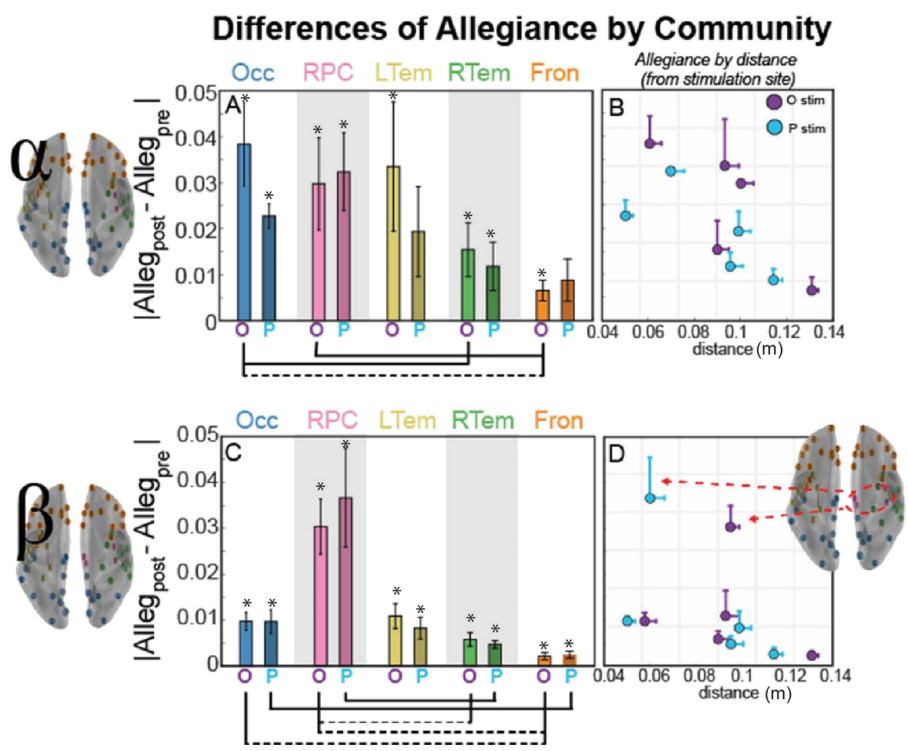

Figure 3. Community allegiance changes within alpha (top) and beta (bottom) band network as a function of distance from the stimulation site. (A, C) Bar plot of the mean magnitude change (SEM across subjects) from the pre-TMS interval in pairwise allegiance from the stimulation site, with the bar labeled O for occipital stimulation and P for parietal stimulation. For paired t test between communities, dotted lines connecting communities indicate uncorrected significance ($p < 0.05$), while solid lines indicate significance corrected for multiple comparisons (Bonferroni, $p < 0.05$). (B, D) Scatter visualization of the mean magnitude allegiance change from the pre-TMS interval shown in Panels A and C, but now plotted as a function of distance from the stimulation site. Error bars indicate SEM across subjects (allegiance) or nodes within the community (distance), and the color of the marker indicates stimulation site (occipital in purple and parietal in blue). Asterisk (*) indicates a significant difference from 0, indicating a change from the pre-TMS interval ($p < 0.05$, uncorrected). Brain inset for the beta band shows the nodes of the RPC community that are most affected by TMS regardless of stimulation site.

subjects within our sample (see Supplemental Figure 6 in the Supporting Information to view more about robustness of effects across subjects). The beta band (bottom row), however, shows clear community specificity, where allegiance of the right paracentral (RPC) community is significantly higher than the right temporal (RTem) and frontal (Fron) communities following stimulation (paired t tests; RTem, $t(9) = -2.6$, $p = 0.028$; Fron, $t(9) = -2.8$, $p = 0.020$, all uncorrected). To speak to robustness, the RPC showed the highest allegiance in 80% and 60% of subjects for occipital and parietal stimulation, respectively. Also, nearly each average change is significantly different from the pre-TMS resting-state estimate (labeled with * in Figure 3A) with the exception of parietal stimulation effects in LTem and Fron.

We also examined whether the community allegiance depended on distance from the stimulation site, which we operationalized as the Euclidean distance from the centroid of the community to the node closest to the stimulation site, estimated in meters from a reconstructed 3D mesh. The effects of stimulation within the alpha band revealed that the nodes closest to the stimulation site are most susceptible to stimulation, and as Figure 3A shows, this effect is reduced for the communities further from the stimulation site (see Supplemental Figure 7 in the Supporting Information for a nonparametric correlational analysis with distance and the graph metrics).

In contrast, the RPC community in the beta band was impacted more strongly by stimulation with high specificity (Figure 3D, pink RPC nodes) by comparison to the other communities. Thus, for the beta band, stimulation didn't follow a simple rule based on distance from the stimulation site as observed in alpha; instead, the stimulation effect was strongest in the RPC community, suggestive of preferred resonant frequencies within the region targeted (Rosanova et al., 2009). This observation aligns with the *natural frequencies* account of stimulation based on the strong role that beta band serves in motor-related activity (Pfurtscheller et al., 1996b), and the prevalence of motor regions within the RPC community. These results also indicate the importance of considering *pairwise* regional activity within a community, so we next examined a network measure of flexibility to investigate regional dynamics.

Flexibility Differences Indicate Whole-Brain Effects Within the Alpha Band

As a complement to allegiance, which measures the temporal consistency of community structure at the interregional level, we investigated flexibility, a metric that describes how often each node changes the community to which it is allied. This analysis captures whether stimulation drives certain brain regions to cohere with different communities in a manner that is different from their community participation prior to stimulation (i.e., network reconfigurations).

Figure 4 shows the differences in flexibility, averaged across nodes within a community, before and after stimulation ($\text{Flex}_{\text{post}} - \text{Flex}_{\text{pre}}$). First, we compared flexibility in these communities to 0, or no difference between $\text{Flex}_{\text{post}}$ and Flex_{pre}. We see that all communities have a significant change in flexibility in both the alpha and the beta communities, suggesting a robust change in flexibility after stimulation reflecting the causal role of TMS pulses on dynamic network reconfigurations. Also, overall, we see a large difference in effect size for the different frequency bands, with alpha communities showing more flexibility overall.

We next compared each community pair to understand the specificity of these effects. Within the alpha band (top row), we observed minimal difference between communities or stimulation sites; rather, TMS is associated with a statistically equivalent change in flexibility across communities. For the beta band (bottom row), a single community stands out. The RPC community is again the most flexible following TMS. For occipital stimulation, flexibility of the right paracentral (RPC) community is significantly higher than the occipital-parietal (Occ) and

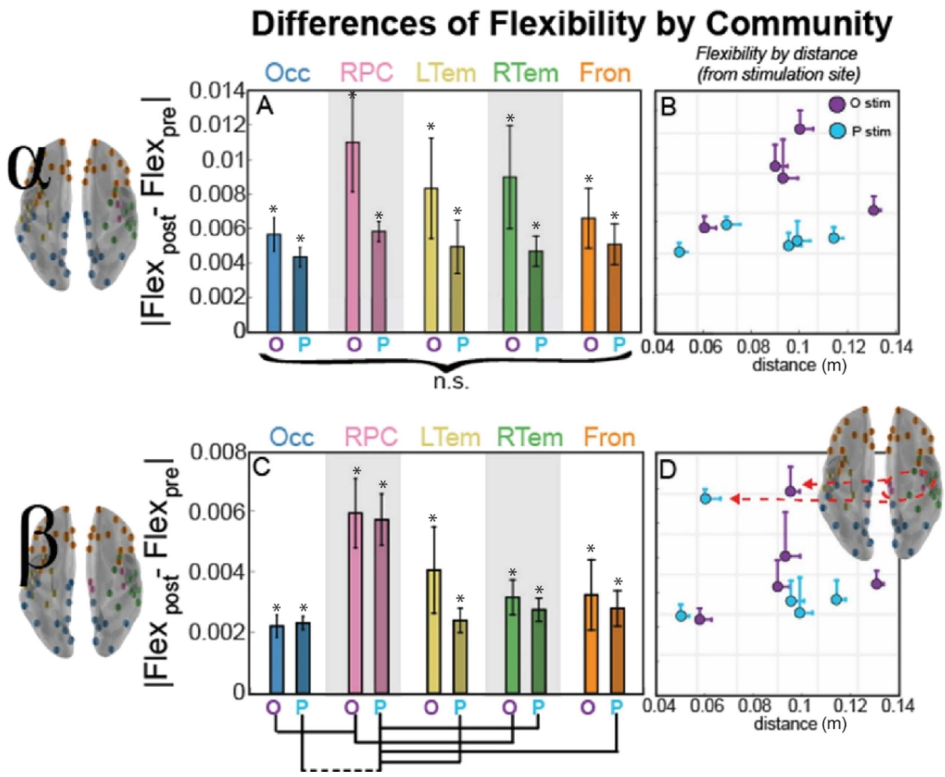

Figure 4. Community flexibility changes within alpha (top) and beta (bottom) band network as a function of distance from the stimulation site. (A, C) Bar plot of the mean magnitude change (SEM across subjects) from the pre-TMS interval in flexibility as a function of the distance from the stimulation site, with the bar labeled O for occipital stimulation and P for parietal stimulation. For paired t test between communities, dotted lines connecting communities indicate uncorrected significance ($p < 0.05$), while solid lines indicate significance corrected for multiple comparisons (Bonferroni, $p < 0.05$). (B, D) Scatterplot of the mean change in flexibility from the pre-TMS interval shown in Panels A and C, but now plotted as a function of distance from the stimulation site. Error bars indicate SEM across subjects (flexibility) or nodes within the community (distance), and the color of the marker indicates stimulation site (occipital in purple and parietal in blue). Asterisk (*) indicates a significant difference from 0, indicating a change from the pre-TMS interval ($p < 0.05$, uncorrected). Brain inset shows the nodes of the RPC community that are most affected by TMS regardless of stimulation site.

trending for right temporal (RTem) communities (paired t tests; Occ, $t(9) = -3.0$, $p = 0.016$, uncorrected; RTem, $t(9) = -2.2$, $p = 0.057$, uncorrected). This difference is even stronger for parietal stimulation, where flexibility for RPC tends to be higher than that observed in the left temporal (LTem), right temporal (RTem), frontal (Fron), and significant (Bonferroni corrected) when compared with occipital-parietal (Occ) communities (paired t tests; LTem, $t(9) = -3.1$, $p = 0.013$; RTem, $t(9) = -2.6$, $p = 0.030$; Fron, $t(9) = -3.1$, $p = 0.014$; Occ, $t(9) = -4.0$, $p = 0.003$, all uncorrected). These results are reminiscent of the pairwise allegiance difference showing an increase within a single community (Figure 5C).

We next examined whether flexibility depended on distance from the stimulation site. Alpha communities showed minimal dependence between distance and flexibility (Figure 4B), but there was no significant difference across any of the communities (Figure 4A). In contrast, when we considered flexibility within the beta band, we observed that the RPC community

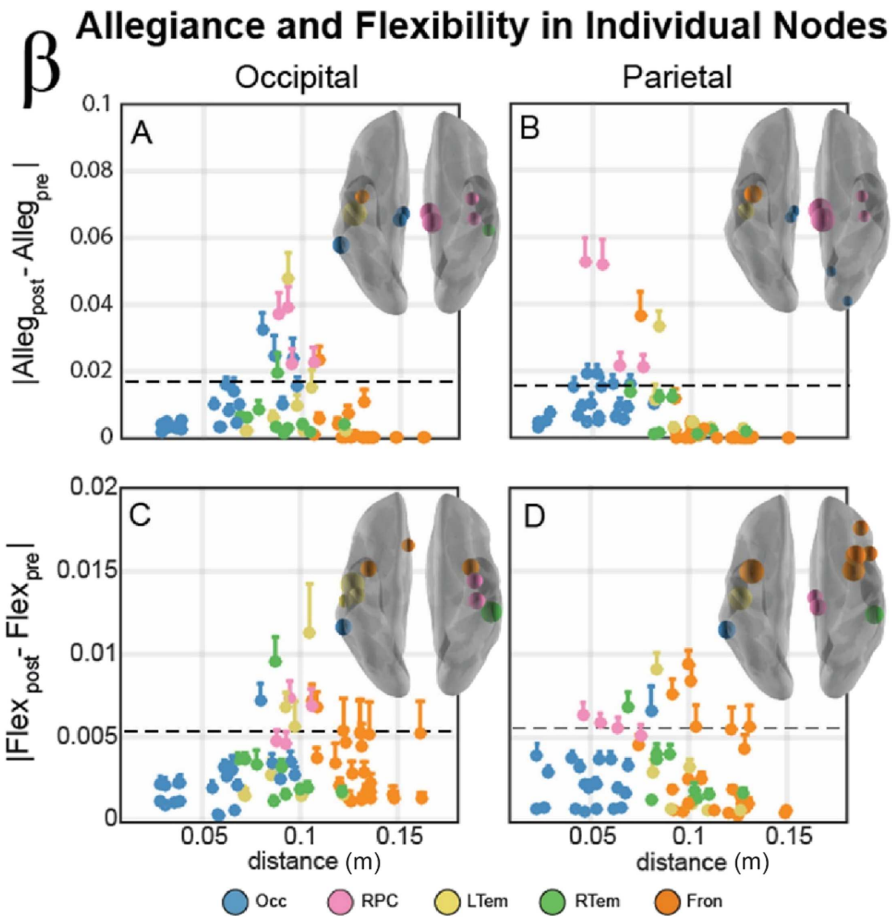

Figure 5. Individual node allegiance (A, B) and flexibility (C, D) changes within the beta band network. (A, B) Individual nodes module allegiance difference ($Alleg_{post} - Alleg_{pre}$) plotted as a function of distance from the stimulation site for occipital (A) and parietal (B) stimulation sites. Color of node describes the community affiliation, and error bars indicate the standard error of the mean. Brain insets display the 85th percentile of module allegiance across all nodes, with nodes scaled by the relative magnitude of this allegiance change. The absolute magnitude of this percentile is also indicated by a horizontal dotted line in each plot. (C, D) Individual nodes flexibility difference ($Flex_{post} - Flex_{pre}$) plotted as a function of distance from the stimulation site for occipital (A) and parietal (B) stimulation sites. Color of nodes, error bars, and brain inset display the same properties as above, but in this panel with flexibility rather than allegiance.

displayed the strongest effect of stimulation (Figure 4D). Combined, these flexibility results demonstrate consistency with the allegiance results, suggesting an effect of resonant frequency in the RPC community for the beta band. However, the communities have variable numbers of nodes, and a few nodes could substantially influence the means shown in Figures 4 and 5, so our final analysis examined individual node dynamics to determine whether the smaller size of the RPC community could be the primary driver of beta band effects.

Individual Node Clusters Suggest a Reconfiguration of the Beta Band Network After TMS

Since all of the previous analyses examined only the overall community differences, our final analysis examined the individual node allegiance to the stimulation site and flexibility changes after stimulation. This analysis examines the spatial specificity of the TMS modification of the

graph metrics that may be masked by averaging across many nodes within the affiliated community. Figure 5 displays individual node magnitude allegiance (top row) and flexibility (bottom row) differences in the five communities of the beta band network following stimulation to occipital (left) and parietal (right) cortex. Overall, there is a change in allegiance within a narrow range of distances from the stimulation site when considering both occipital (Figure 5A) and parietal stimulation (Figure 5B). Although regions in the right paracentral community (RPC, pink) show substantial change in allegiance, several nodes from other communities also have a similar response profile. To examine the spatial topology of these effects, the brain insets illustrate nodes corresponding to the top 15% of allegiance changes (nodes on or above the threshold line in Figure 5A–B). The most influenced nodes surround the sensorimotor regions of the brain, including the RPC community and nearby regions around the central sulcus, the rolandic sites of the brain.

In contrast, the individual node flexibility changes are more diffuse (Figure 5, bottom row). The nodes corresponding to the top 15% of flexibility changes are plotted above the threshold line, and these effects span a larger range of distances than the allegiance changes. However, the spatial topology is quite similar. Changes in flexibility after stimulation are strongest in a cluster of nodes surrounding the central sulcus. Collectively, these results reveal that the nodes in the RPC community were not uniquely influenced; instead, the network dynamics of the RPC as well as the surrounding bilateral sensorimotor regions showed the largest flexibility and allegiance changes within the beta band communities. Together these results suggest a rapid *reconfiguration* of the resting beta community organization following TMS stimulation, rather than enhancement of a single community.

DISCUSSION

We investigated network reconfiguration in resting-state EEG following single pulses of transcranial magnetic stimulation (TMS) using a method from network science that allows for a quantitative description of the brain's modular architecture (Bassett & Bullmore, 2006; Bullmore & Sporns, 2012; Ercsey-Ravasz et al., 2013). Our analysis focused on connectivity differences between the 1 s before stimulation and the 1 s after stimulation. More specifically, we examined network differences in the alpha and beta frequency bands since these bands have been suggested as resonant frequencies within the stimulated regions: alpha in occipital and beta in parietal regions (Laufs et al., 2003; Rosanova et al., 2009).

Our results first examined whole-brain effects of stimulation, and we observed differential effects on connectivity according to stimulation site, although more subtle differentiation was seen between the alpha and beta frequency bands as very similar data-driven network structures were derived from each band. We employed a network theoretical approach to identify communities from the resting-state EEG data, and importantly, we observed several differences in the structure of functional connectivity in each frequency band following TMS. Within the alpha band, stimulation produced local effects, but interestingly, also produced more global effects as evidenced by modification of network flexibility across all *occipital, parietal, paracentral, and frontal* communities when TMS was applied to either occipital or parietal cortex. In stark contrast, beta band activity showed high specificity of TMS-induced effects on allegiance and flexibility within a rather focal paracentral network near sensorimotor cortex, regardless of stimulation site. These novel results using network science approaches with TMS-EEG revealed an interesting interplay between local and global activity across frequency bands that might underlie how network reconfigurations give rise to coordinated brain activity.

Global Effects Within the Alpha Band Manifest in Similar Flexibility Across Communities

We have shown that TMS to resonating communities constrained within the alpha band has a similar impact on the overall flexibility of each community. This finding implies a global impact of stimulation, regardless of stimulation site, to the alpha band networks. Since the first observations of the alpha band by Berger (1929), alpha band activity (8–12 Hz), also known as the Berger rhythm, has been a brain rhythm of frequent study because of its dominance in resting EEG, and it is often the only visually observable pattern to the naked eye in the EEG trace. Since its first observation, several hypotheses have been proposed ascribing a functional role to its presence in EEG. The first theory was proposed by Adrian and Matthews (1934), who found that the power within the alpha band increases when subjects are awake with eyes closed. They interpreted this as alpha band activity reflecting a brain state of inactivity, priming the brain for incoming information. This theory has been expanded and revised to more clearly represent "cortical idling" (Pfurtscheller, Stancák, & Neuper, 2006a). Recently, however, this theory has been somewhat abandoned because of the difficulty of reconciling it with behavioral experiments that indicate a functional role for power within this band. For example, alpha band activity is also associated with working memory load (Jensen, Gelfand, Kounios, & Lisman, 2002; Klimesch, 1996; Tuladhar et al., 2007). Thus, beyond this "spontaneous" alpha rhythm, researchers have discovered other forms of alpha, so-called functional alpha (Başar, 2012), which is observed during many cognitive and motor processes. These theories have been further broadened, suggesting that alpha activity may even be an access controller to a knowledge system (Klimesch, 2012). Collectively, however, alpha activity consistently represents a diffuse, communicative signal with multiple functions, an arguably global signal in terms of its impact on sensory information.

Research using TMS to investigate the functional connectivity within the alpha band, however, provides a more limited view of alpha activity. For example, Rosanova et al. (2009) showed that enhancement of the alpha band is primarily restricted to occipital cortex, regardless of stimulation site. These researchers noted that occipital cortex might even resonate at the alpha frequency. Our results expand the theory proposed by Rosanova and colleagues by showing that the brain may be parsed into separate resonating communities within the alpha band and that each cluster is overall equally modified by TMS, as indicated by the similar flexibility metrics across the resonating communities. Interestingly, however, nodal allegiance to the stimulation site reveals a rather direct and localized impact within the occipital and parietal cortex: specifically, the cluster that is the most spatially proximal to the stimulation site and previously associated with alpha band activity (i.e., the bilateral occipital-parietal network, Occ). Together, these results suggest a process whereby alpha connectivity can provide both the specific visual effects shown in early studies while also serving many functional roles across disparate brain regions.

Local Effects of Beta Band Manifest in the Specificity of Network Changes Within the Paracentral Community

Two pieces of evidence in the current study converge to show that the paracentral network plays a highly specific role in dynamic network reconfiguration within the beta band, and our results support and extend the natural frequency theory of the brain following single pulses of TMS (Rosanova et al., 2009). First, the network communities defined on resting-state activity are identical between alpha and beta bands, except for the right paracentral network (RPC). The beta band RPC consists of nodes within the paracentral lobule and two nodes within the pre- and postcentral gyri that play a predominant role in sensorimotor processing, consistent with previous research that has identified motor-related activity in the beta band

(Pfurtscheller et al., 1996b). Second, following a single TMS pulse to either stimulation site, we observe that the paracentral region uniquely displays both the highest flexibility and allegiance changes from the baseline state in the beta band, but not the alpha band. Together, these findings suggest a unique specificity that would support the natural frequency theory of TMS and are aligned with other network metrics suggesting beta band influence after parietal stimulation (Amico et al., 2017). In fact, our results provide intuition at a level of granularity that has not been previously explored, by capitalizing on recently developed methods from network science (Bassett & Sporns, 2017) to investigate perturbations of brain networks following single pulses of TMS.

The granularity of this effect was further enhanced by inspection of the nodal allegiance and flexibility across the brain. The RPC community was clearly involved and appeared to be an isolated community with increased nodal allegiance (among its nodes) and global flexibility in the beta band communities. However, when we inspected the single nodes contributing to this effect, we found that this effect was not constrained by the boundaries of the beta band RPC network as we defined from baseline activity. Instead, the effects spread to nodes outside this RPC community and consisted of a cluster of nodes surrounding the central sulcus. This granularity of the beta band network effects after TMS aligns well with the well-known involvement of rolandic sites in sensorimotor processes and discharges of beta band activity (Baker, 2007).

Clinical Implications

TMS has been used successfully in clinical settings for treating movement disorders (Pascual-Leone et al., 1994) and mitigating severe affective disorders (Berman et al., 2000); however, some studies that have investigated the efficacy and efficiency of TMS treatment for depression (for review, Loo & Mitchell, 2005) suggest that most treatment regimens are suboptimal, often stimulating for a duration of two weeks and having only a minor benefit. Here we have shown a complex interplay between local and global neural processing, but more generally, our results speak to the specificity of TMS, where particular resonating communities of brain regions (e.g., beta band activity emanating from sensorimotor regions) or diffuse sets of resonating communities (e.g., all regions in alpha band) may be modified by TMS regardless of stimulation site. In other words, we show that stimulating a focal region can have distal effects on many other brain regions. Future studies expanding on how individual variability in brain connectivity impacts how TMS propagates through cortex may eventually reveal the specific networks or brain regions that may predict successful treatment. We believe the methods and initial results within this work hold promise in future studies to help determine stimulation protocols for a variety of clinical settings and surrounding several cognitive domains.

Our results first examined whole-brain effects of stimulation, and we observed differential effects on connectivity in both alpha and beta activity, although no stark differentiation was seen between stimulation to occipital or parietal sites, globally. Next, we employed a network theoretical approach to identify communities from the resting-state EEG data, and we observed several differences in the structure of functional connectivity in both frequency bands after TMS. Within the alpha band, stimulation produced local effects, but interestingly, stimulation also produced more global effects, altering network flexibility across all communities when applied to either occipital or parietal cortex.

Despite these general effects, our coarse-level results are merely the first step, as much more must be completed to determine the robustness of much of these network dynamics that may include any gender differences (70% of this sample were male), individual susceptibility to stimulation, or state-based stimulation specificity (Thut et al., 2011), of which our current

study does not tackle. We further expand on other methodological considerations that may guide future studies within this domain in the following.

Methodological Considerations

Our use of community detection to understand functional connectivity in the brain and the effects of TMS on specific brain networks focuses on two stimulation sites and two common frequency bands. We use a phase-based undirected connectivity measurement and inspect graph metric changes at a single snapshot of the available parameters within the dynamic modularity framework we applied. This initial implementation of a graph theoretical approach on human neurostimulation effects may be expanded in the future to investigate the directed communication between these resonating communities (e.g., Reimann et al., 2017), cross-frequency communication (Canolty & Knight, 2010), and increased resolution across frequencies of the brain. The methodological choices within this work also focused on merely one spatiotemporal scale, which may not completely account for the spectral sensitivity across the regions of the brain, and the results target a wakeful resting state in individuals, and it may not extend to the active or sleeping brain (Hasson, Nusbaum, & Small, 2009; Massimini et al., 2005). Future research may extend this work to take into account the spectral macroarchitecture of evoked and induced oscillations in the brain.

Our experimental design did not employ neuronavigation or a control stimulation site; instead, our participants completed four experimental sessions across four different days to maximize the variability in the prestimulation period to identify stimulation effects robust to state differences (boredom, fatigue, mind wandering, etc.). However, an interesting avenue for future work would be to examine network changes that may be more closely tied to functionally localized regions, where neuronavigation would serve a critical role in equating more precise stimulation locations between individuals. Similarly, our analysis did not require a control site since our investigation examined changes between baseline activity and activity following stimulation. The debate on how to "control" for neurostimulation techniques has recently received increased attention. Research using simultaneous TMS-EEG studies often have non-stimulation-related evoked activity (i.e., the auditory "click"; Conde et al., 2019); however, there is also a debate on how the researchers implemented their controls (Belardinelli et al., 2019). This debate is essential for studies that directly examine the neural activity following stimulation; however, our design attempted to overcome the challenge of non-stimulation-related evoked activity by comparing conditions where these nuisance signals are nearly equated. Thus, our investigation examined changes between baseline activity and activity following stimulation and presents an alternative to this debate within the context of two stimulation sites. The analytic logic we employed in our analysis follows the classic comparison logic between conditions in traditional neuroimaging analysis: Conditions are designed to only manipulate the factor of interest, so looking at their difference eliminates all of the concomitant neural processing that occurs but is tangential to condition comparison of interest. Here, the analysis statistically examined differences from a baseline period but also qualitatively between occipital and parietal stimulation, so each served as the other's control for nuisance signals that are concurrent but tangential to the stimulation effects. A similar logic could apply to the experimental design decision to not include an explicit control for the auditory click sound from the TMS pulse. Although participants wore ear plugs to mitigate the sensory response in auditory cortex, the focus on relative differences between stimulation sites should help eliminate the effect of the auditory response on the results since it is expected that the sensory effect is equivalent across the conditions. Our results, for the connectivity measurement, clearly differentiate the stimulation sites; in contrast, it should be noted that the

network metrics rarely differentiate stimulation sites. The auditory click could still contribute to the observed network effects, but given the stimulation site specificity of the connectivity matrices, it is likely to be a small contributor. However, future research could examine any of these inferences/assumptions in greater detail. In particular, investigations may use more regions and intensities to augment our understanding about differences in ongoing activity with more functionally determined stimulation protocols.

Conclusion

Using a recently developed network-based methodology applied to EEG, we have investigated the reconfigurations of naturally resonating communities of brain regions. While the alpha network reveals the dynamic interplay of local and global activity, communities within the beta band revealed a remarkable specificity, displaying more local connectivity changes. Particularly important next steps include linking these observations with emerging theories of the impact of stimulation on distributed networks in the form of network control theory (Gu et al., 2015), which has begun to offer insights into the brain's preference for certain low-energy states (Betzel et al., 2017), the role that brain topology plays on the energy required for brain state transitions (Kim et al., in press; Tang & Bassett, in press), and the predicted impact of stimulation on distal areas (Gu et al., in press; Muldoon et al., 2016). Efforts to ground TMS studies like the one we report here in a mechanistic theory could have lasting consequences in studies linking behavioral changes to neural oscillations or neurostimulation (Medaglia et al., in press), but may also impact future protocols for clinical purposes, providing a means to reconfigure resonating clusters in the brain.

MATERIALS AND METHODS

Participants

Ten individuals (seven men, three women, aged 20–33, M = 23.8, $SD = 4.8$) participated in the TMS-EEG experiment. All gave informed, written consent as approved by the University of California, Irvine, Institutional Review Board.

TMS-EEG Data Collection

Data collection occurred in the TMS-EEG Laboratory in the Human Neuroscience Lab at the University of California, Irvine. The subjects were seated in a comfortable chair approximately 60 cm from the monitor, equipped with earplugs to attenuate the sound of the coil discharge, and their heads were fixed in a chin rest to minimize movement while they continuously fixated on the center of the monitor screen. No overt motor responses were required during the 30-min experimental session.

Stimulation was applied with a MagStim Model 200 Monophasic Stimulator P/N 3010-00 equipped with a figure-of-eight coil at 55% stimulator intensity (E-field 297 V/m). We established this intensity in a previous study that had a similar protocol (Garcia et al., 2011) by systematically modulating the intensity threshold since motor thresholds are inappropriate for occipital stimulation (Stewart, Walsh, & Rothwell, 2001). We found that only 37% of participants saw a phosphene at approximately 70%. Thus, we set the stimulation intensity for this study to be at 55% of stimulation (20% less than the phosphene induction threshold). We targeted four regions that included symmetric areas in occipital and parietal cortices (Figure 6), and the location for these regions was estimated by electrodes O1/O2 and P1/P2 of the 10-20 international scheme for EEG. This method reliably targets a similar area across participants within 2 cm of sulcal/gyral landmarks (Herwig, Satrapi, & Schönfeldt-Lecuona, 2003), the

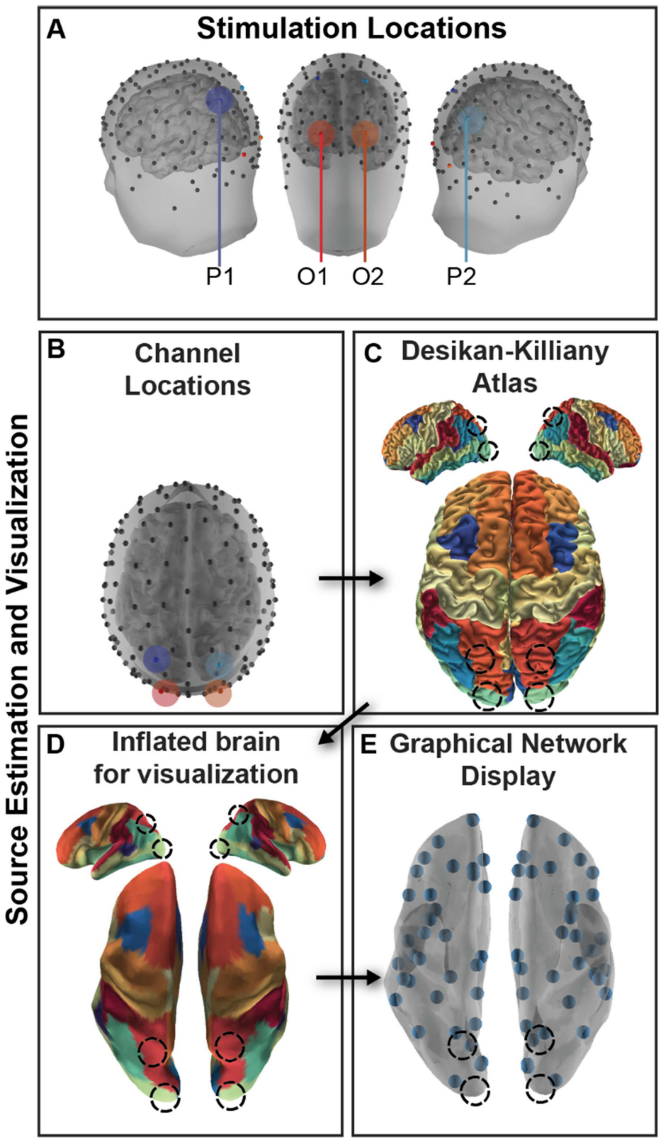

Figure 6. Experimental design and analysis. (A) Participants received stimulation in symmetric regions in occipital (O1, O2) and parietal (P1, P2) cortex. (B) High-density EEG recorded from 128 channels was submitted to a cLORETA source analysis, and current source density (CSD) was estimated for each vertex of a high-resolution mesh. (C) CSD was then averaged within a parcellation of cortex following the Desikan-Killiany atlas parcellation to estimate regional brain activity. (D) The cortex was inflated for visualization. (E) Each centroid of the region is plotted as a small orb. Stimulation locations marked in each visualization with a shaded region or a dotted line.

resolution of high-density EEG used in this study. For occipital stimulation, the coil was oriented parallel to the coronal view (i.e., paddle pointed up), and for parietal stimulation, the coil was oriented approximately tangential to the curvature of the scalp at the electrode target locations (i.e., paddle pointed back and down). For each region, participants completed a block of approximately 100 single pulses of stimulation that were no closer than 4 s apart (jittered up to 6 s apart), following standard safety procedures (Rossi, Hallett, Rossini, & Pascual-Leone, 2009). Within a session, the 10 blocks were semi-randomly selected among the four stimulation

sites (O1, O2, P1, P2), ensuring that multiple blocks of each stimulation type occurred in each session. Participants complete four sessions (one subject participated in five) on separate days, providing an aggregate of approximately 4,000 total stimulation trials for each subject; however, one subject completed an additional session and another subject terminated one session because of fatigue.

Throughout the session, 128 channels of EEG were recorded using a TMS-compatible EEG system from Advanced Neuro Technology (ANT, The Netherlands). The Waveguard cap system consisted of small Ag/AgCl electrode elements, specially designed to yield high-quality and stable recordings with simultaneous TMS. EEG data were sampled at 1024 Hz for this experiment and impedances were targeted to be kept below 10 kΩ.

EEG Analysis

Segmentation of epochs. The EEG data were preprocessed following an established pipeline (Garcia et al., 2011) for each of the four sessions for each of the 10 participants. First, raw EEG were submitted to a principal component analysis (PCA) to identify the peak amplitude events that correspond to the stimulation event and to eliminate any timing discrepancy between the intended and actual timing of the stimulation pulse in the EEG data. After the timing of each pulse was recovered, the decomposition was discarded and was not used in any subsequent analysis (i.e., no components were removed). Using the maxima from the largest component of each dataset as the onset of stimulation, the collected datasets were segmented into approximately 40,000 epochs that were 6 s in duration, including 3 s (3,072 samples) before and after the TMS pulse. After this segmentation procedure, the four samples before the pulse and 16 (15.6 ms) after the pulse were removed from the epochs to remove artifacts from the amplifier. These samples were later replaced with a forward autoregressive moving average prediction of the contaminated data from the intervals directly preceding the TMS pulse and a mild Savitzky-Golay smoothing filter over the interval surrounding the pulse to remove any quick shifts in amplitude due to the artifact editing procedure. Finally, each trial was normalized by the standard deviation of the 512 samples prior to the stimulation so that each subject contributed similarly to grand mean TMS-evoked potentials (TEPs); however, this did not have an impact on the overall shape of the TEP (see Supporting Information Figures). Because of the known multiple sources of artifacts in work using simultaneous TMS-EEG (Rogasch & Fitzgerald, 2013) beyond the amplifier artifacts within the 20 samples (19.5 ms), aggressive means were used to ensure artifact was eliminated from our estimates. Automated artifact editing based on amplitude thresholds was used. The thresholding procedure used a percentile rank of epochs within the data. Ranks were calculated based on the maximum fluctuation found in the raw EEG response on each trial for each electrode. In turn, trials were discarded if the maximum response in 15% of electrodes was greater than the 95th percentile compared with all other trials. This eliminated approximately 30% of trials likely contaminated with artifacts from the TMS pulse or blink artifacts, leaving the following trial total for analysis in the participants: 3,129, 1,768, 3,535, 4,021, 2,269, 2,308, 2,931, 2,032, 2,840, and 3,088. After this preliminary preprocessing, we largely followed the PREP approach, an artifact-removal procedure that has been shown to be robust to artifacts within high-artifact environments (Bigdely-Shamlo, Mullen, Kothe, Su, & Robbins, 2015). The following steps were completed: (a) line noise removal via a frequency-domain (multitaper) regression technique to remove 60 Hz and harmonics present in the signal; (b) a robust average reference with a Huber mean; (c) artifact subspace reconstruction to remove residual artifacts with the standard deviation cutoff parameter set to 15; and (d) band-pass filtering using a Butterworth filter with 2-dB attenuation at 2 and 50 Hz. TEPs may be seen in Supplemental Figures 2, 4, and 5 in the Supporting Information, displaying how the preprocessing pipeline has successfully removed these data.

Distributed source reconstruction: The method by which we may estimate neural activity from specific locations in the brain but measured from the scalp.

Distributed source reconstruction. From the preprocessed EEG data, we estimated current source density (CSD) over a 5,003-vertex cortical mesh. A boundary element method (BEM) forward model was derived from the Colin 27 anatomy (Holmes et al., 1998) and transformed into MNI305 space (Evans et al., 1993) using standard electrode positions fit to the Colin 27 head surface in Brainstorm (Tadel, Baillet, Mosher, Pantazis, & Leahy, 2011). The BEM solution was computed using OpenMEEG (Gramfort, Papadopoulo, Olivi, & Clerc, 2010; Kybic et al., 2005), and the cLORETA approach was used for inverse modeling as described in detail in Mullen et al. (2015) and implemented in the BCILAB (Kothe & Makeig, 2013) and Source Information Flow (Mullen, 2014) toolboxes. Then CSD was averaged into one time course from each of the 68 regions of the Desikan-Killiany atlas (Desikan et al., 2006) and downsampled to 128 Hz for use in the connectivity analysis. As a final step after parcellation, the surface mesh of the Colin 27 brain (with DK atlas parcellated regions) was imported into Matlab and distance was estimated between regions closest to the stimulation site (bilateral lateral occipital and superior parietal) and every other region in the DK atlas using pdist.m in Matlab. For community "distance," the average distance from the stimulation site was estimated, corresponding to centroid distance of the community.

Functional Connectivity Analysis

To estimate functional connectivity of brain networks before and after stimulation, an undirected measure, known as the debiased weighted phase lag index (dwPLI), was computed between each pair of the 68 estimated brain regions from the atlas. DwPLI is robust against the influence of volume conduction, uncorrelated noise, and intersubject variations in sample size (Vinck et al., 2011; Vindiola et al., 2014), and it has previously been proposed to be an appropriate pairing with a source localization analysis to minimize the influence of these nuisance variables (Hillebrand, Barnes, Bosboom, Berendse, & Stam, 2012; van Diessen et al., 2015).

The connectivity estimates were calculated using Matlab and FieldTrip (Oostenveld, Fries, Maris, & Schoffelen, 2010). First, a multitaper spectral estimation was applied to the CSD measurements, and then dwPLI was computed between all source pairs to estimate the functional connectivity pattern of signals in the frequency range between 2 Hz and 25 Hz (step = 0.5 Hz) in a 5-s window centered on the stimulation pulse (−2.5 s to 2.5 s). The dwPLI connectivity estimates were calculated across trials, representing the trial-by-trial consistency between regional CSD. Next the matrix of dwPLI estimates was reduced to the 51 time windows corresponding to windows centered 38 ms apart, from 1 s before the TMS pulse to 1 s after the TMS pulse. Since this estimate was done using a Hanning windowing method, the windows are not independent and represent some smearing in time.

Dynamic community detection: A process that distills complex connectivity matrices into a series of cluster labels related to how nodes coalesce into a network and change across time.

Dynamic Community Detection

In addition to looking at whole-brain connectivity patterns, we employed a community detection algorithm (Bassett & Bullmore, 2006; Bullmore & Sporns, 2012; Ercsey-Ravasz et al., 2013) to examine whether regions formed modular networks, and whether the regional composition of these networks changed before and after stimulation across the 51 time windows in our 2-s epoch. The algorithm optimizes a multilayer modularity quality function, Q, using a Louvain-like greedy algorithm (Blondel et al., 2008; Mucha et al., 2010) to assign brain regions to communities. The community assignments are dependent on two parameters: (a) a structural resolution γ parameter and (b) a temporal resolution ω parameter. These two parameters determine the scale of the resulting graph, both structurally and temporally, and here,

we sweep this parameter space to find the scale of the data that is most unlike that expected in an appropriate random network null model. As described in Garcia et al. (2018), there are several heuristics we may use to determine the optimal parameter for our dataset. We chose an unbiased "difference" heuristic because of the unique properties of this stimulation dataset, which we explain below.

Following our previous work on fMRI data (Bassett et al., 2013), the values for both parameters were determined by comparing the mean value of Q in the experimental data to the mean value of Q in a shuffled null model of the data; we tested a very wide range of values for each parameter since this algorithm has not yet been applied to EEG data, which have inherently different temporal and spatial scales of functional connectivity (Nunez & Srinivasan, 2006). Our analysis examined parameters for $\gamma = 0.8$ to $\gamma = 1.6$ and $\omega = 0.5$ to $\omega = 35$. The null model of the data was created by randomly shuffling the pairwise dwPLI values, destroying the correlational structure observed in EEG data for each subject and parameter pairing. Each Q was then subtracted for each parameter pairing, comparing the observed model's Q (from the unperturbed EEG connectivity patterns) and the null model's Qnull (shuffled connectivity patterns) for each subject. Our analysis found a clear peak in the resulting Q matrix, suggesting that the range used was appropriate for this dataset. In fact, the largest difference was found for $\gamma = 1.025$ and $\omega = 9$, and these parameters were used in the reported analyses, which suggests that the temporal parameter (ω) is the parameter that captures the unique properties of the EEG signal. Since the community detection algorithm is nondeterministic (Good, de Montjoye, & Clauset, 2010), 100 iterations of the hard partitions were estimated with modularity maximization for each subject and stimulation condition (O1, O2, P1, P2), yielding 100 sets of community labels for the 68 nodes for each of the four stimulation conditions for each of the 10 subjects.

Community metrics. Within each of the 51 time windows of our 2-s stimulation epoch, we examined the relationship among the brain regions within a community to characterize the dynamic reconfiguration of spatially distributed neural sources before and after stimulation. Our analysis investigated two community metrics, flexibility (Bassett et al., 2011) and allegiance (Bassett et al., 2015). Figure 7 is a visual depiction of the steps needed to estimate these community metrics.

The flexibility of each node corresponds to the number of instances in which a node changes community affiliation, g, normalized by the total possible number of changes that could occur across the layers L (Bassett et al., 2011), which represents each time slice within this dynamic community detection algorithm. In other words, the flexibility of a single node i, ξ_i, may be estimated with the following:

$$\xi_i = \frac{g_i}{L-1}, \tag{1}$$

where L is the total number of temporal windows.

Allegiance estimates how much regions communicate with subnetworks in the community structure and demonstrate the same pattern of connectivity across time points. We define allegiance matrix P, where edge weight P_{ij} denotes the number of times a pair of nodes moves to the same community together divided by $L - 1$ possible changes.

Thus, allegiance increases the resolution of community and captures coordinated activity of each node with every other node in the brain, whereas flexibility examines whether a brain region changes affiliations overall.

Each of these measures was calculated twice, once for the 25 windows of partitions before TMS (pre-TMS) and once for the 25 windows following TMS (post-TMS), ignoring the center window where stimulation occurred. Our analysis focused on the absolute difference in

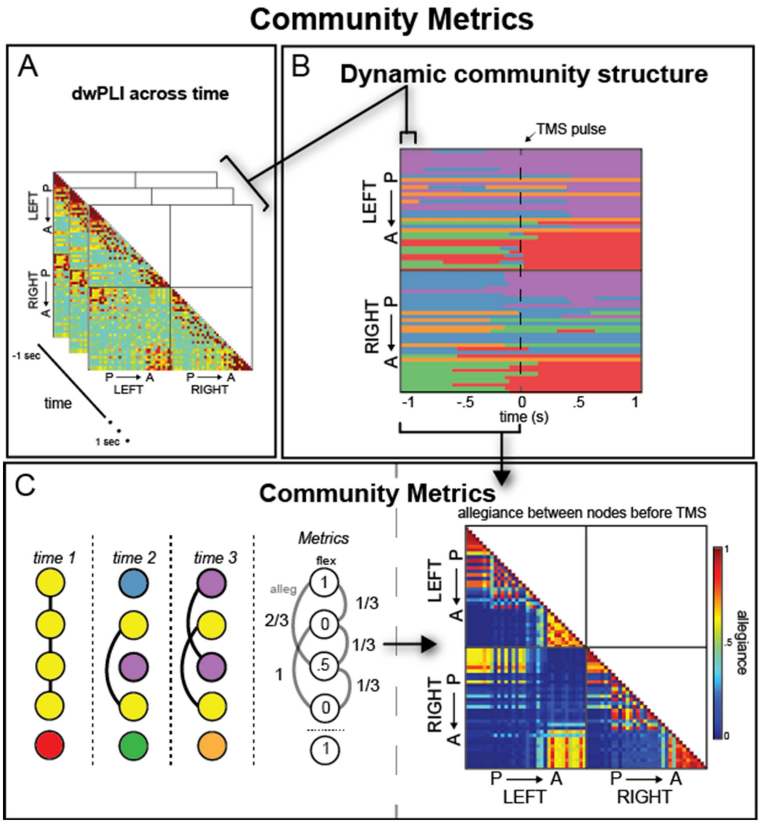

Figure 7. Overview of analysis method and natural brain architecture. (A) DwPLI was estimated across trials in 40-ms windows across the 2-s epoch, including 1 s before and 1 s after the TMS onset (P: posterior, A: anterior nodes). (B) Dynamic network communities from a sample subject derived from the dwPLI estimate for each window. Each color marks a different community label. (C, left) From Panel B, community metrics were calculated that represent how often a node changes over time (flexibility) or how often each node pair is in the same community over time (allegiance). The cartoon networks show five hypothetical nodes that change communities over time (three time windows shown). Connections are marked as black lines and metrics are given in the final column, showing a range of flexibility and allegiance values. These metrics are used in subsequent analyses. (C, right) Summary allegiance matrix for a sample subject for the period before TMS onset, indicating the natural architecture of connectivity within the alpha band.

allegiance and flexibility between pre-TMS and post-TMS communities, emphasizing whether stimulation influences local or global brain dynamics more strongly.

Finally, results were averaged across left and right stimulation sites since we were interested in the general magnitude of changes from functionally similar regions. In support of this data reduction primarily driven by our broad interest in coarse parietal/occipital stimulation differences, follow-on analyses did not show any differences in consistency of network changes between left and right stimulation, using a temporal consensus method inspired by Doron, Bassett, & Gazzaniga (2012) in Supplemental Figure 8 (see the Supporting Information).

Statistical Analyses

To find the substantial changes in metrics across the pre-TMS and post-TMS intervals, traditional linear statistics were used, where the pre-TMS and post-TMS intervals were treated as conditions and paired-sample t tests were applied to node or communities or a one-sample

t test of differences (for the dwPLI comparison) from 0, as indicated in the text. In cases where multiple comparisons were carried out (e.g., Figures 1 and 3), a Bonferroni correction or false discovery rate was used to determine significance. For the Bonferroni correction, each band-specific metric was treated as a separate set of tests (10 comparisons within a set, Community 1 vs. Community 2, Community 1 vs. Community 3, etc.), so the corrected alpha value was set to 0.005. For the false discovery rate, p values were adjusted within each dwPLI matrix (Figure 1), and as reported $q < 0.05$ was used. Where appropriate, both the corrected and uncorrected significant comparisons are shown (see Figures 3 and 4).

ACKNOWLEDGMENTS

The authors acknowledge thoughtful discussions with our colleagues at the University of California, Irvine, for study coordination and subject testing. This research was supported by mission funding to the Army Research Laboratory as well as sponsored by the Army Research Laboratory and accomplished under Cooperative Agreement Number W911NF-10-2-0022. We would also like to acknowledge that the work was partially collected while J. O. G. was funded by a National Research Service Award (F31-EY-019241) awarded by the National Institutes of Health. The views and conclusions contained in this document are those of the authors and should not be interpreted as representing the official policies, either expressed or implied, of the Army Research Laboratory or the U.S. Government.

SUPPORTING INFORMATION

Supporting information for this article is available at https://doi.org/10.1162/netn_a_00139.

AUTHOR CONTRIBUTIONS

Javier Omar Garcia: Conceptualization; Formal analysis; Methodology; Visualization; Writing-Original Draft; Writing - Review & Editing. Arian Ashourvan: Formal analysis; Methodology; Writing - Review & Editing. Steven M. Thurman: Validation; Writing - Original Draft. Ramesh Srinivasan: Conceptualization; Data curation; Methodology; Resources; Writing - Review & Editing. Danielle Bassett: Conceptualization; Formal analysis; Methodology; Writing - Original Draft; Writing - Review & Editing. Jean Vettel: Conceptualization; Methodology; Writing - Original Draft; Writing - Review & Editing.

FUNDING INFORMATION

Army Research Laboratory (http://dx.doi.org/10.13039/100006754), Award ID: W911NF-10-2-0022.

REFERENCES

Achard, S., Salvador, R., Whitcher, B., Suckling, J., & Bullmore, E. (2006). A resilient, low-frequency, small-world human brain functional network with highly connected association cortical hubs. *Journal of Neuroscience*, *26*, 63–72. https://doi.org/10.1523/jneurosci.3874-05.2006

Adrian, E. D., & Matthews, B. H. C. (1934). The interpretation of potential waves in the cortex. *Journal of Physiology*, *81*, 440–471.

Alivisatos, A. P., Chun, M., Church, G. M., Greenspan, R. J., Roukes, M. L., & Yuste, R. (2012). The Brain Activity Map Project and the challenge of functional connectomics. *Neuron*, *74*, 970–974. https://doi.org/10.1016/j.neuron.2012.06.006

Amico, E., Bodart, O., Rosanova, M., Gosseries, O., Heine, L., Van Mierlo, P., . . . , Laureys, S. (2017). Tracking dynamic interactions between structural and functional connectivity: A TMS/EEG-dMRI study. *Brain Connectivity*, *7*, 84–97. https://doi.org/10.1089/brain.2016.0462

Ashourvan, A., Gu, S., Mattar, M. G., Vettel, J. M., & Bassett, D. S. (2017). The energy landscape underpinning module dynamics in the human brain connectome. *NeuroImage*, *157*, 364–380. https://doi.org/10.1016/j.neuroimage.2017.05.067

Auriat, A. M., Neva, J. L., Peters, S., Ferris, J. K., & Boyd, L. A. (2015). A review of transcranial magnetic stimulation and multimodal neuroimaging to characterize post-stroke neuroplasticity.

Frontiers in Neurology, 6. https://doi.org/10.3389/fneur.2015.00226

Azevedo, F. A. C., Carvalho, L. R. B., Grinberg, L. T., Farfel, J. M., Ferretti, R. E. L., Leite, R. E. P., . . . , Herculano-Houzel, S. (2009). Equal numbers of neuronal and nonneuronal cells make the human brain an isometrically scaled-up primate brain. *Journal of Comparative Neurology*, *513*, 532–541. https://doi.org/10.1002/cne.21974

Baker, S. N. (2007). Oscillatory interactions between sensorimotor cortex and the periphery. *Current Opinion in Neurobiology*, *17*, 649–655. https://doi.org/10.1016/j.conb.2008.01.007

Başar, E. (2012). A review of alpha activity in integrative brain function: Fundamental physiology, sensory coding, cognition and pathology. *International Journal of Psychophysiology*, *86*, 1–24. https://doi.org/10.1016/j.ijpsycho.2012.07.002

Başar, E., Başar-Eroğlu, C., Karakaş, S., & Schürmann, M. (1999). Are cognitive processes manifested in event-related gamma, alpha, theta and delta oscillations in the EEG? *Neuroscience Letters*, *259*, 165–168. https://doi.org/10.1016/S0304-3940(98)00934-3.

Bassett, D. S., & Bullmore, E. (2006). Small-world brain networks. *Neuroscientist*, *12*, 512–523. https://doi.org/10.1177/1073858406293182

Bassett, D. S., Porter, M. A., Wymbs, N. F., Grafton, S. T., Carlson, J. M., & Mucha, P. J. (2013). Robust detection of dynamic community structure in networks. *Chaos*, *23*, 013142. https://doi.org/10.1063/1.4790830

Bassett, D. S., & Sporns, O. (2017). Network neuroscience. *Nature Neuroscience*, *20*, 353–364. https://doi.org/10.1038/nn.4502

Bassett, D. S., Wymbs, N. F., Porter, M. A., Mucha, P. J., Carlson, J. M., & Grafton, S. T. (2011). Dynamic reconfiguration of human brain networks during learning. *Proceedings of the National Academy of Sciences*, *108*, 7641–7646. https://doi.org/10.1073/pnas.1018985108

Bassett, D. S., Yang, M., Wymbs, N. F., & Grafton, S. T. (2015). Learning-induced autonomy of sensorimotor systems. *Nature Neuroscience*, *18*, 744–751. https://doi.org/10.1038/nn.3993

Belardinelli, P., Biabani, M., Blumberger, D. M., Bortoletto, M., Casarotto, S., David, O., . . . Ilmoniemi, R. J. (2019). Reproducibility in TMS–EEG studies: A call for data sharing, standard procedures and effective experimental control. Brain Stimulation: Basic. *Translational, and Clinical Research in Neuromodulation*, *12*, 787–790. https://doi.org/10.1016/j.brs.2019.01.010

Benjamini, Y., & Yekutieli, D. (2001). The control of the false discovery rate in multiple testing under dependency. *Annals of Statistics*, *29*, 1165–1188. https://doi.org/10.1214/aos/1013699998

Berger, H. (1929). Electroencephalogram in humans. *Archiv für Psychiatrie und Nervenkrankheiten*, *87*, 527–570. https://doi.org/10.1007/BF01797193

Bergmann, T. O., Karabanov, A., Hartwigsen, G., Thielscher, A., & Siebner, H. R. (2016). Combining non-invasive transcranial brain stimulation with neuroimaging and electrophysiology: Current approaches and future perspectives. *NeuroImage*, *140*, 4–19. https://doi.org/10.1016/j.neuroimage.2016.02.012

Berman, R. M., Narasimhan, M., Sanacora, G., Miano, A. P., Hoffman, R. E., Hu, X. S., . . . Boutros, N. N. (2000). A randomized clinical trial of repetitive transcranial magnetic stimulation in the treatment of major depression. *Biological Psychiatry*, *47*, 332–337. https://doi.org/10.1016/S0006-3223(99)00243-7

Bestmann, S., Ruff, C. C., Blankenburg, F., Weiskopf, N., Driver, J., & Rothwell, J. C. (2008). Mapping causal interregional influences with concurrent TMS–fMRI. *Experimental Brain Research*, *191*, 383. https://doi.org/10.1007/s00221-008-1601-8

Betzel, R. F., Satterthwaite, T. D., Gold, J. I., & Bassett, D. S. (2017). Positive affect, surprise, and fatigue are correlates of network flexibility. *Scientific Reports*, *7*, 520. https://doi.org/10.1038/s41598-017-00425-z

Bigdely-Shamlo, N., Mullen, T., Kothe, C., Su, K.-M., & Robbins, K. A. (2015). The PREP pipeline: Standardized preprocessing for large-scale EEG analysis. *Frontiers in Neuroinformatics*, *9*, 16. https://doi.org/10.3389/fninf.2015.00016

Blondel, V. D., Guillaume, J.-L., Lambiotte, R., & Lefebvre, E. (2008). Fast unfolding of communities in large networks. *Journal of Statistical Mechanics*, *2008*, P10008. https://doi.org/10.1088/1742-5468/2008/10/P10008

Bohning, D., Shastri, A., McConnell, K., Nahas, Z., Lorberbaum, J., Roberts, D., . . . George, M. S. (1999). A combined TMS/fMRI study of intensity-dependent TMS over motor cortex. *Biological Psychiatry*, *45*, 385–394. https://doi.org/10.1016/S0006-3223(98)00368-0

Bortoletto, M., Veniero, D., Thut, G., & Miniussi, C. (2015). The contribution of TMS–EEG coregistration in the exploration of the human cortical connectome. *Neuroscience and Biobehavioral Reviews*, *49*, 114–124. https://doi.org/10.1016/j.neubiorev.2014.12.014

Braun, U., Schäfer, A., Walter, H., Erk, S., Romanczuk-Seiferth, N., Haddad, L., . . . Bassett,D. S. (2015). Dynamic reconfiguration of frontal brain networks during executive cognition in humans. *Proceedings of the National Academy of Sciences*, *112*, 11678–11683. https://doi.org/10.1073/pnas.1422487112

Bressler, S. L., & Kelso, J. A. S. (2001). Cortical coordination dynamics and cognition. *Trends in Cognitive Sciences*, *5*, 26–36. https://doi.org/10.1016/S1364-6613(00)01564-3

Bressler, S. L., & Menon, V. (2010). Large-scale brain networks in cognition: Emerging methods and principles. *Trends in Cognitive Sciences*, *14*, 277–290. https://doi.org/10.1016/j.tics.2010.04.004

Brunel, N., & Wang, X.-J. (2003). What determines the frequency of fast network oscillations with irregular neural discharges? I. Synaptic dynamics and excitation-inhibition balance. *Journal of Neurophysiology*, *90*, 415–430. https://doi.org/10.1152/jn.01095.2002

Brunoni, A. R., & Vanderhasselt, M.-A. (2014). Working memory improvement with non-invasive brain stimulation of the dorsolateral prefrontal cortex: A systematic review and meta-analysis. *Brain and Cognition*, *86*, 1–9. https://doi.org/10.1016/j.bandc.2014.01.008

Bullmore, E., & Sporns, O. (2012). The economy of brain network organization. *Nature Reviews Neuroscience*, *13*, 336–349. https://doi.org/10.1038/nrn3214

Buzsáki, G. (2006). *Rhythms of the brain*. New York, NY: Oxford University Press.

Buzsáki, G., & Draguhn, A. (2004). Neuronal oscillations in cortical networks. *Science*, *304*, 1926–1929. https://doi.org/10.1126/science.1099745

Buzsáki, G., & Wang, X. J. (2012). Mechanisms of gamma oscillations. *Annual Review of Neuroscience*, *35*, 203–225. https://doi.org/10.1146/annurev-neuro-062111-150444

Canolty, R. T., & Knight, R. T. (2010). The functional role of cross-frequency coupling. *Trends in Cognitive Sciences*, *14*, 506–515. https://doi.org/10.1016/j.tics.2010.09.001

Cocchi, L., Gollo, L. L., Zalesky, A., & Breakspear, M. (2017). Criticality in the brain: A synthesis of neurobiology, models and cognition. *Progress in Neurobiology*, *158*, 132–152. https://doi.org/10.1016/j.pneurobio.2017.07.002

Cocchi, L., Sale, M. V., Lord, A., Zalesky, A., Breakspear, M., & Mattingley, J. B. (2015). Dissociable effects of local inhibitory and excitatory theta-burst stimulation on large-scale brain dynamics. *Journal of Neurophysiology*, *113*, 3375–3385. https://doi.org/10.1152/jn.00850.2014

Conde, V., Tomasevic, L., Akopian, I., Stanek, K., Saturnino, G. B., Thielscher, A., . . . Siebner, H. R. (2019). The non-transcranial TMS-evoked potential is an inherent source of ambiguity in TMS-EEG studies. *NeuroImage*, *185*, 300–312. https://doi.org/10.1016/j.neuroimage.2018.10.052

Desikan, R. S., Ségonne, F., Fischl, B., Quinn, B. T., Dickerson, B. C., Blacker, D., . . . Killiany, R. J. (2006). An automated labeling system for subdividing the human cerebral cortex on MRI scans into gyral based regions of interest. *NeuroImage*, *31*, 968–980. https://doi.org/10.1016/j.neuroimage.2006.01.021

Doron, K. W., Bassett, D. S., & Gazzaniga, M. S. (2012). Dynamic network structure of interhemispheric coordination. *Proceedings of the National Academy of Sciences*, *109*, 18661–18668. https://doi.org/10.1073/pnas.1216402109

Driver, J., Blankenburg, F., Bestmann, S., Vanduffel, W., & Ruff, C. C. (2009). Concurrent brain-stimulation and neuroimaging for studies of cognition. *Trends in Cognitive Sciences*, *13*, 319–327. https://doi.org/10.1016/j.tics.2009.04.007

Eldaief, M. C., Press, D. Z., & Pascual-Leone, A. (2013). Pascual-leone, A Transcranial magnetic stimulation in neurology. *Neurology Clinical Practice*, *3*, 519–526. https://doi.org/10.1212/01.CPJ.0000436213.11132.8e

Ercsey-Ravasz, M., Markov, N. T., Lamy, C., Van Essen, D. C., Knoblauch, K., Toroczkai, Z., & Kennedy, H. (2013). A predictive network model of cerebral cortical connectivity based on a distance rule. *Neuron*, *80*, 184–197. https://doi.org/10.1016/j.neuron.2013.07.036

Evans, A. C., Collins, D. L., Mills, S. R., Brown, E. D., Kelly, R. L., & Peters, T. M. (1993). 3D statistical neuroanatomical models from 305 MRI volumes. *1993 IEEE Conference Record Nuclear Science Symposium and Medical Imaging Conference*, *3*, 1813–1817. https://doi.org/10.1109/NSSMIC.1993.373602

Fries, P., Nikolić, D., & Singer, W. (2007). The gamma cycle. *Trends in Neurosciences*, *30*, 309–316. https://doi.org/10.1016/j.tins.2007.05.005

Garcia, J. O., Ashourvan, A., Muldoon, S., Vettel, J. M., & Bassett, D. S. (2018). Applications of community detection techniques to brain graphs: Algorithmic considerations and implications for neural function. *Proceedings of the IEEE*, *106*, 846–867. https://doi.org/10.1109/JPROC.2017.2786710

Garcia, J. O., Grossman, E. D., & Srinivasan, R. (2011). Evoked potentials in large-scale cortical networks elicited by TMS of the visual cortex. *Journal of Neurophysiology*, *106*, 1734–1746. https://doi.org/10.1152/jn.00739.2010

Geisler, C., Brunel, N., & Wang, X.-J. (2005). Contributions of intrinsic membrane dynamics to fast network oscillations with irregular neuronal discharges. *Journal of Neurophysiology*, *94*, 4344–4361. https://doi.org/10.1152/jn.00510.2004

Gollo, L. L., Roberts, J. A., & Cocchi, L. (2017). Mapping how local perturbations influence systems-level brain dynamics. *NeuroImage*, *160*, 97–112. https://doi.org/10.1016/j.neuroimage.2017.01.057

Good, B. H., de Montjoye, Y.-A., & Clauset, A. (2010). Performance of modularity maximization in practical contexts. *Physical Review E*, *81*, 046106. https://doi.org/10.1103/PhysRevE.81.046106

Gramfort, A., Papadopoulo, T., Olivi, E., & Clerc, M. (2010). OpenMEEG: Opensource software for quasistatic bioelectromagnetics. *BioMedical Engineering OnLine*, *9*, 45. https://doi.org/10.1186/1475-925X-9-45

Gu, S., Cieslak, M., Baird, B., Muldoon, S. F., Grafton, S. T., Pasqualetti, F., & Bassett, D. S. (in press). The energy landscape of neurophysiological activity implicit in brain network structure. *NeuroImage*. Retrieved from https://arxiv.org/abs/1607.01959

Gu, S., Pasqualetti, F., Cieslak, M., Telesford, Q. K., Yu, A. B., Kahn, A. E., . . . Bassett, D. S. (2015). Controllability of structural brain networks. *Nature Communications*, *6*, ncomms9414. https://doi.org/10.1038/ncomms9414

Hari, R. & Salmelin, R. (1997). Human cortical oscillations: A neuromagnetic view through the skull. *Trends in Neurosciences*, *20*, 44–49. https://doi.org/10.1016/S0166-2236(96)10065-5

Hasson, U., Nusbaum, H. C., & Small, S. L. (2009). Task-dependent organization of brain regions active during rest. *Proceedings of the National Academy of Sciences*, *106*, 10841–10846. https://doi.org/10.1073/pnas.0903253106

Herring, J. D., Thut, G., Jensen, O., & Bergmann, T. O. (2015). Attention modulates TMS-locked alpha oscillations in the visual cortex. *Journal of Neuroscience*, *35*, 14435–14447. https://doi.org/10.1523/JNEUROSCI.1833-15.2015

Herwig, U., Satrapi, P., & Schönfeldt-Lecuona, C. (2003). Using the international 10-20 EEG system for positioning of transcranial magnetic stimulation. *Brain Topography*, *16*(2), 95–99.

Hillebrand, A., Barnes, G. R., Bosboom, J. L., Berendse, H. W., & Stam, C. J. (2012). Frequency-dependent functional connectivity within resting-state networks: An atlas-based MEG beamformer solution. *NeuroImage*, *59*, 3909–3921. https://doi.org/10.1016/j.neuroimage.2011.11.005

Holmes, C. J., Hoge, R., Collins, L., Woods, R., Toga, A. W., & Evans, A. C. (1998). Enhancement of MR images using registration for signal averaging. *Journal of Computer Assisted Tomography*, *22*, 324–333.

Ilmoniemi, R. J., Virtanen, J., Ruohonen, J., Karhu, J., Aronen, H. J., Näätänen, R., & Katila, T. (1997). Neuronal responses to magnetic stimulation reveal cortical reactivity and connectivity.

Neuroreport, *8*, 3537–3540. https://doi.org/10.1097/00001756-199711100-00024

Jensen, O., Gelfand, J., Kounios, J., & Lisman, J. E. (2002). Oscillations in the alpha band (9–12 Hz) increase with memory load during retention in a short-term memory task. *Cerebral Cortex*, *12*, 877–882.

Kim, J., Soffer, J. M., Kahn, A. E., Vettel, J. M., Pasqualetti, F., & Bassett, D. S. (in press). Topological principles of control in dynamical network systems. *Nature Physics*. Retrieved from http://arxiv.org/abs/1702.00354

Klimesch, W. (1996). Memory processes, brain oscillations and EEG synchronization. *International Journal of Psychophysiology*, *24*, 61–100. https://doi.org/10.1016/S0167-8760(96)00057-8

Klimesch, W. (2012). Alpha-band oscillations, attention, and controlled access to stored information. *Trends in Cognitive Sciences*, *16*, 606–617. https://doi.org/10.1016/j.tics.2012.10.007

Kothe, C. A., & Makeig, S. (2013). BCILAB: A platform for brain-computer interface development. *Journal of Neural Engineering*, *10*, 056014. https://doi.org/10.1088/1741-2560/10/5/056014

Kybic, J., Clerc, M., Abboud, T., Faugeras, O., Keriven, R., & Papadopoulo, T. (2005). A common formalism for the integral formulations of the forward EEG problem. *IEEE Transactions on Medical Imaging*, *24*, 12–28. https://doi.org/10.1109/TMI.2004.837363

Laufs, H., Kleinschmidt, A., Beyerle, A., Eger, E., Salek-Haddadi, A., Preibisch, C., et al. (2003). EEG-correlated fMRI of human alpha activity. *NeuroImage*, *19*(4), 1463–1476.

Loo, C. K., & Mitchell, P. B. (2005). A review of the efficacy of transcranial magnetic stimulation (TMS) treatment for depression, and current and future strategies to optimize efficacy. *Journal of Affective Disorders*, *88*(3), 255–267.

Mancini, M., Mastropasqua, C., Bonnì, S., Ponzo, V., Cercignani, M., Conforto, S., . . . Bozzali, M. (2017). Theta burst stimulation of the precuneus modulates resting state connectivity in the left temporal pole. *Brain Topography*, *30*, 312–319. https://doi.org/10.1007/s10548-017-0559-x

Massimini, M., Ferrarelli, F., Huber, R., Esser, S. K., Singh, H., & Tononi, G. (2005). Breakdown of cortical effective connectivity during sleep. *Science*, *309*, 2228–2232. https://doi.org/10.1126/science.1117256

Massimini, M., Tononi, G., & Huber, R. (2009). Slow waves, synaptic plasticity and information processing: Insights from transcranial magnetic stimulation and high-density EEG experiments. *European Journal of Neuroscience*, *29*, 1761–1770. https://doi.org/10.1111/j.1460-9568.2009.06720.x

Medaglia, J. D., Huang, W., Karuza, E. A., Thompson-Schill, S. L., Ribeiro, A., & Bassett, D. S. (in press). Functional alignment with anatomical networks is associated with cognitive flexibility. *Nature Human Behavior*. Retrieved from https://arxiv.org/abs/1611.08751

Mucha, P. J., Richardson, T., Macon, K., Porter, M. A., & Onnela, J. P. (2010). Community structure in time-dependent, multiscale, and multiplex networks. *Science*, *328*, 876–878.

Muldoon, S. F., Pasqualetti, F., Gu, S., Cieslak, M., Grafton, S. T., Vettel, J. M., & Bassett, D. S. (2016). Stimulation-based control of dynamic brain networks. *PLoS Computational Biology*, *12*, e1005076. https://doi.org/10.1371/journal.pcbi.1005076

Mullen, T. R. (2014). *The dynamic brain: Modeling neural dynamics and interactions from human electrophysiological recordings* (doctoral dissertation). Retrieved from https://escholarship.org/uc/item/7kk2c4nd

Mullen, T. R., Kothe, C. A. E., Chi, Y. M., Ojeda, A., Kerth, T., Makeig, S., . . . Cauwenberghs, G. (2015). Real-time neuroimaging and cognitive monitoring using wearable dry EEG. *IEEE Transactions on Biomedical Engineering*, *62*, 2553–2567. https://doi.org/10.1109/TBME.2015.2481482

Nunez, P. L., & Srinivasan, R. (2006). *Electric fields of the brain: The neurophysics of EEG*. New York, NY: Oxford University Press.

Nunez, P. L., Wingeier, B. M., & Silberstein, R. B. (2001). Spatial-temporal structures of human alpha rhythms: Theory, microcurrent sources, multiscale measurements, and global binding of local networks. *Human Brain Mapping*, *13*, 125–164. https://doi.org/10.1002/hbm.1030

Oostenveld, R., Fries, P., Maris, E., & Schoffelen, J.-M. (2010). FieldTrip: Open source software for advanced analysis of MEG, EEG, and invasive electrophysiological data. *Computational Intelligence and Neuroscience*, *2011*, e156869. https://doi.org/10.1155/2011/156869

Pascual-Leone, A., Valls-Solé, J., Brasil-Neto, J. P., Cammarota, A., Grafman, J., & Hallett, M. (1994). Akinesia in Parkinson's disease. II. Effects of subthreshold repetitive transcranial motor cortex stimulation. *Neurology*, *44*, 892–898.

Pascual-Leone, A., Walsh, V., & Rothwell, J. (2000). Transcranial magnetic stimulation in cognitive neuroscience—virtual lesion, chronometry, and functional connectivity. *Current Opinion in Neurobiology*, *10*, 232–237. https://doi.org/10.1016/S0959-4388(00)00081-7

Paus, T. (1998). Imaging the brain before, during, and after transcranial magnetic stimulation. *Neuropsychologia*, *37*, 219–224. https://doi.org/10.1016/S0028-3932(98)00096-7

Pfurtscheller, G., Stancák, A., & Neuper, C. (2006a). Event-related synchronization (ERS) in the alpha band—An electrophysiological correlate of cortical idling: A review. *International Journal of Psychophysiology*, *24*, 39–46.

Pfurtscheller, G., Stancák, A., Jr., & Neuper, C. (1996b). Post-movement beta synchronization. A correlate of an idling motor area? *Electroencephalography and Clinical Neurophysiology*, *98*, 281–293. https://doi.org/10.1016/0013-4694(95)00258-8

Reimann, M. W., Nolte, M., Scolamiero, M., Turner, K., Perin, R., Chindemi, G., . . . Markram, H. (2017). Cliques of neurons bound into cavities provide a missing link between structure and function. *Front. Comput. Neurosci.*, 11. https://doi.org/10.3389/fncom.2017.00048

Rogasch, N. C., & Fitzgerald, P. B. (2013). Assessing cortical network properties using TMS-EEG. *Human Brain Mapping*, *34*, 1652–1669. https://doi.org/10.1002/hbm.22016

Romei, V., Murray, M. M., Cappe, C., & Thut, G. (2013). The contributions of sensory dominance and attentional bias to cross-modal enhancement of visual cortex excitability. *Journal of Cognitive Neuroscience*, *25*, 1122–1135. https://doi.org/10.1162/jocn_a_00367

Romei, V., Thut, G., Mok, R. M., Schyns, P. G., & Driver, J. (2012). Causal implication by rhythmic transcranial magnetic stimulation of alpha frequency in feature-based local vs. global attention.

European Journal of Neuroscience, *35*, 968–974. https://doi.org/10.1111/j.1460-9568.2012.08020.x

Rosanova, M., Casali, A., Bellina, V., Resta, F., Mariotti, M., & Massimini, M. (2009). Natural frequencies of human corticothalamic circuits. *Journal of Neuroscience*, *29*, 7679–7685. https://doi.org/10.1523/jneurosci.0445-09.2009

Rose, N. S., LaRocque, J. J., Riggall, A. C., Gosseries, O., Starrett, M. J., Meyering, E. E., & Postle, B. R. (2016). Reactivation of latent working memories with transcranial magnetic stimulation. *Science*, (354)1136–1139. https://doi.org/10.1126/science.aah7011

Rossi, S., Hallett, M., Rossini, P. M., & Pascual-Leone, A. (2009). Safety, ethical considerations, and application guidelines for the use of transcranial magnetic stimulation in clinical practice and research. *Clinical Neurophysiology*, *120*, 2008–2039. https://doi.org/10.1016/j.clinph.2009.08.016

Sale, M. V., Mattingley, J. B., Zalesky, A., & Cocchi, L. (2015). Imaging human brain networks to improve the clinical efficacy of non-invasive brain stimulation. *Neuroscience and Biobehavioral Reviews*, *57*, 187–198. https://doi.org/10.1016/j.neubiorev.2015.09.010

Siebner, H. R., Bergmann, T. O., Bestmann, S., Massimini, M., Johansen-Berg, H., Mochizuki, H., . . . Rossini, P. M. (2009). Consensus paper: Combining transcranial stimulation with neuroimaging. *Brain Stimulation*, *2*, 58–80. https://doi.org/10.1016/j.brs.2008.11.002

Sporns, O., Chialvo, D. R., Kaiser, M., & Hilgetag, C. C. (2004). Organization, development and function of complex brain networks. *Trends in Cognitive Sciences*, *8*, 418–25. https://doi.org/10.1016/j.tics.2004.07.008

Stewart, L. M., Walsh, V., & Rothwell, J. C. (2001). Motor and phosphene thresholds: A transcranial magnetic stimulation correlation study. *Neuropsychologia*, *39*, 415–419.

Tadel, F., Baillet, S., Mosher, J. C., Pantazis, D., & Leahy, R. M. (2011). Brainstorm: A user-friendly application for MEG/EEG analysis. *Computational Intelligence and Neuroscience*, *2011*, e879716. https://doi.org/10.1155/2011/879716

Tang, E., & Bassett, D. S. (in press). Control of dynamics in brain networks. *Nature Communications*. Retrieved from https://arxiv.org/abs/1701.01531

Taylor, P. C. J., & Thut, G. (2012). Brain activity underlying visual perception and attention as inferred from TMS–EEG: A review. *Brain Stimulation*, *5*, 124–129.

Telesford, Q. K., Lynall, M.-E., Vettel, J., Miller, M. B., Grafton, S. T., & Bassett, D. S. (2016). Detection of functional brain network reconfiguration during task-driven cognitive states. *NeuroImage*, *142*, 198–210. https://doi.org/10.1016/j.neuroimage.2016.05.078

Thut, G., Veniero, D., Romei, V., Miniussi, C., Schyns, P., & Gross, J. (2011). hythmic TMS causes local entrainment of natural oscillatory signatures. *Current Biology*, *21*, 1176–1185. https://doi.org/10.1016/j.cub.2011.05.049

Tuladhar, A. M., ter Huurne, N., Schoffelen, J.-M., Maris, E., Oostenveld, R., & Jensen, O. (2007). Parieto-occipital sources account for the increase in alpha activity with working memory load. *Human Brain Mapping*, *28*, 785–792. https://doi.org/10.1002/hbm.20306

van Diessen, E., Numan, T., van Dellen, E., van der Kooi, A. W., Boersma, M., Hofman, D., . . . Stam, C. J. (2015). Opportunities and methodological challenges in EEG and MEG resting state functional brain network research. *Clinical Neurophysiology*, *126*, 1468–1481. https://doi.org/10.1016/j.clinph.2014.11.018

Vinck, M., Oostenveld, R., van Wingerden, M., Battaglia, F., & Pennartz, C. M. A. (2011). An improved index of phase-synchronization for electrophysiological data in the presence of volume-conduction, noise and sample-size bias. *Neuro Image*, *55*, 1548–65. https://doi.org/10.1016/j.neuroimage.2011.01.055

Vindiola, M. M., Vettel, J. M., Gordon, S. M., Franaszczuk, P. J., & McDowell, K. (2014). Applying EEG phase synchronization measures to non-linearly coupled neural mass models. *Journal of Neuroscience Methods*, *226*, 1–14. https://doi.org/10.1016/j.jneumeth.2014.01.025

Volberg, G., Kliegl, K., Hanslmayr, S., & Greenlee, M. W. (2009). EEG alpha oscillations in the preparation for global and local processing predict behavioral performance. *Human Brain Mapping*, *30*, 2173–2183. https://doi.org/10.1002/hbm.20659